Fleet Tracker

A Technical Report for ECE 4440

Presented to the Faculty of the School of Engineering and Applied Sciences
University of Virginia • Charlottesville, Virginia

In Partial Fulfillment of the Requirements for the Degree
Bachelor of Science in Computer Engineering

Author

Nojan Sheybani
December 16, 2019

Technical Project Team Members

Jesse Dugan
Nayiri Krzysztofowicz
Vivian Lin
Malcolm Miller

On my honor as a University Student, I have neither given nor received unauthorized aid on this assignment as defined by the Honor Guidelines for Thesis-Related Assignments

Signature _____ Date _____

Approved _____ Date _____
Rider Foley, Department of Engineering and Society

Statement of work

Jesse Dugan

My primary role was the design and construction of the hardware. This consisted of designing the schematics, laying out and routing the printed circuit boards (PCBs), creating a bill of materials (BOM), ordering all components, and soldering some sections for the home and roaming nodes. For the final project, we made three PCBs: one home node and two roaming nodes. I made both schematics in Multisim using the custom footprints that Nayiri created. I then did the layout and routing for each board in Ultiboard. With Malcolm's help, I ensured that all parts of the boards were easy to test by adding header pins, jumpers, and debugging LEDs.

When the boards arrived, I took them to WWW Electronics Inc. (3W) to have the small (0402) components and the integrated circuit (IC) chips soldered. I soldered the larger components (0805), the header pins and sockets, the connectors, and the test pins. Finally, I tested the boards using a digital multimeter (DMM), oscilloscope, and spectrum analyzer. I also tested the power system first using a power supply and then by monitoring its performance in direct sunlight using the LabVIEW VI that Malcolm created.

Nayiri Krzysztofowicz

My primary role for this project was to design the user interface (UI) to display the information received by the home node. I wrote a program in Python that received the packet from the home node via universal asynchronous receiver-transmitter (UART), extracted all relevant information, and drew the global positioning system (GPS) coordinates on a map interface and displayed the timestamp.

I also helped Jesse with the board design by creating all custom symbols and footprints for the schematic and layout for all parts not included in Multisim. I also updated the user database to contain all necessary information for each part such as part numbers, availability, and price.

Vivian Lin

My primary role for this project was to implement the protocols for data transfer. The first protocol was the reliable data transport (RDT) protocol, for which I updated the existing base code that Jesse and I had already created as part of a separate project. As part of this, I altered the handshake procedure and the data transfer procedure to accommodate the possibility of two roaming nodes transmitting to the home node at once. The second protocol was the multiple access control (MAC) protocol, which handled the possibility of collisions when multiple nodes were transmitting data on the single channel. I implemented the protocol along the existing guidelines of Carrier Sense Multiple Access with Collision Avoidance.

Besides the protocol section of the firmware, I implemented a basic duty cycling scheme on the roaming nodes to conserve power and worked extensively with the LoRa transceiver. I also worked with Nojan and Nayiri to integrate our distinct modules, the GPS code, the protocol code, and the user interface code. With Nojan, I worked on constructing the packet payload, containing GPS and timestamp data. I communicated with Nayiri to ensure that she had enough information about the firmware to integrate her user interface code without errors.

Malcolm Miller

My primary role for this project was the power system of our roaming node. However, I contributed to various components of our project throughout the semester. For the midterm

design review, I created the energy budget. This consisted of calculating the longevity of our battery. In these calculations, I took into account battery degradation, power harvested from our solar panel (in various lighting conditions), the power modes of our GPS module and MSP microcontroller, and the power draw of our LoRa transceiver. For LoRa power draw calculations, I worked alongside Vivian to compute the probability of a failed transmission. Additionally, I used the time over air metric to determine the configuration settings (e.g., spreading factor) to optimize range and the probability of a successful transmission. Following these calculations, I designed the structure of the payload to be sent over LoRa. Using fixed point representations, I was able to store all necessary data (e.g., latitude, time of transmission) in 15 bytes of data.

Other contributions include assisting in the design of firmware to both configure the GPS and extract pertinent values (latitude, longitude, date, and time) from the received packet. Additionally, I contributed to the selection of components and the schematic designs for each of the boards. Finally, I designed and implemented a real-time power and energy analysis program using LabVIEW. This software obtains ADC readings using a myRIO, applies an averaging filter to reduce noise, and performs energy calculations using trapezoidal approximation.

Nojan Sheybani

My primary role for this project was the general firmware for our system, especially setting up the GPS to collect data and communicate with the MSP430 microcontroller. This consisted of configuring SPI communications between the MSP430 and the GPS, configuring the GPS, figuring out how to send multi-byte commands from the MSP430 to the GPS, and deciding the sequences of commands that must be sent to retrieve time and location data from the GPS.

Upon consistent and successful reception of a packet from the GPS, I worked on extracting the important data, such as longitude, latitude, and day, and fitting those values into a 15-byte payload for easy integration with the LoRa code that Vivian worked on.

Originally, my secondary role was software, but Nayiri expertly handled the software side and we decided that it was not a complex enough effort to warrant two people working on it. Instead of working on the software, I worked alongside Vivian to test and integrate the LoRa and GPS code to finalize our end-to-end system. Upon successful integration, I assisted with a breadth of end-to-end testing of our system to ensure that our project works correctly with more than one roaming node and at varying ranges.

Abstract

Dugan's Dogs' final capstone project is a self-powered GPS tracking system ideal for deployment in rural areas. It attaches to any sun-exposed vehicle and relays the vehicle's GPS location (latitude and longitude) in real-time to a central node, which displays the location on an interactive map. The project involves a star network of two roaming nodes that communicate with a central home node. The roaming nodes are self-powered by solar energy and communicate through LoRa (long range) modulation and a reliable data transport (RDT) network protocol. A media access control (MAC) protocol that uses channel activity detection (CAD) and exponential back-off ensures that all nodes communicate without interference. This project joins many other self-powered Internet of Things (IoT) applications at the forefront of recent research and commercial products.

Background

The rise of the Internet of Things (IoT) has revolutionized the way we monitor systems. Through the use of distributed sensors and vast communication networks, the IoT provides connectivity and intelligence to our daily lives [1]. Current applications of the IoT include industry, agriculture, and health, among several others [2]. However, reliance on cellular networks and primary cell (non-rechargeable) batteries limit IoT applications in rural America [3].

Low Power Wide Area Network (LPWAN) protocols such as LoRa (long range) are an emerging alternative to cellular networks. LoRa can operate independently of existing infrastructure, providing a long range, low power solution suitable for rural deployment [4]. LoRa is conducive to solar energy harvesting, which provides reliable off-grid power without the replacement needs of a primary cell battery [5]. Use of alternative network protocols and a self-powered system provides a framework for reliable IoT application in rural communities. Team Dugan's Dogs has applied this framework to create a solar-powered GPS tracking system, the Fleet Tracker. The system is designed for use on school buses, but can be extended to other tracking applications such as farm equipment.

Similar GPS tracking systems exist in academic research and the commercial sector. Da Silva *et al*. [3] created a battery-powered tracking system using LoRa protocol, with a high success rate of transmissions and high accuracy of GPS data. The Fleet Tracker system expands on their work by integrating renewable energy to create a self-powered system. Many commercial fleet trackers exist, and most connect to cellular networks. A popular example is the Samsara AG24 low-power fleet tracker. It is battery-powered, uses solar panels as a backup power source, and uses a SIM card to connect to 4G LTE [6]. This increases power consumption and decreases rural reliability. The Fleet Tracker system uses a similar power system, but will use less power and provide increased reliability in rural areas that lack cellular service.

The team's GPS tracking system builds upon the material the team members learned throughout their undergraduate careers. The idea was inspired by the special topics course "Self-powered systems design for the Internet of Things" that several team members took this semester. The board designs build upon the information from the FUN series regarding schematic design, board layout, and routing. The firmware uses many techniques learned in Introduction to Embedded, as well as a few learned in Advanced Embedded. The reliable data transfer protocol is an implementation of a technique learned in Computer Networks, and Communications helped the team members understand the fundamentals of modulation. However, LoRa was not covered in Communications, and has required much outside research. Finally, the data visualization incorporates skills learned in Advanced Software Development.

Constraints

Design Constraints

Since the Dugan's Dogs team consists of a mix of computer and electrical engineers, two main constraints were placed upon the design by the capstone course itself. First, the project had to include a microcontroller or a National Instruments myRIO [7], and secondly it had to include a custom printed circuit board that the team designed itself.

CPU Limitations

The Texas Instruments MSP430F5529 [8] microcontroller was chosen as the CPU based off of the multiple peripheral interfaces and the large amount of GPIO pins. The clock speed was limited to 1 MHz to conserve power. This also limited the peripheral clocks, such as for the serial peripheral interface (SPI) lines, to 1 MHZ.

Software Availability

National Instruments' Multisim [9] and Ultiboard [10] tools were required for board design, as UVA has active licenses to use those tools. Additionally, Code Composer Studio [11] was used for the embedded code, as it is free and compatible with the selected microcontroller.

Manufacturing Limitations

Manufacturing constraints were imposed by the PCB manufacturer, Advanced Circuits, to qualify for the student special for four-layer boards. The 4-layer boards were required to have a thickness of 62 mils, with a 39-mil core. This affected the RF section and is discussed further in the Detailed Technical Description: Hardware: PCB Design section of this report. The most pertinent constraints [12] to this project were:

- Maximum board size: 30 square inches
- Minimum 5 mil line/space
- Minimum 10 mil hole size
- Maximum 50 drilled holes per square inch

To minimize costs, the roaming nodes were panelized, which limited their sizes to less than 15 square inches each.

Additionally, WWW Electronics Inc., who helped populate the PCBs, was unable to solder certain packages such as ball grid array (BGA). BGA was the only package available for the GPS module, so the GPS was included as a header board.

Economic and Cost Constraints

The budget for this project was a few hundred dollars per team. This meant that large amounts of backup components could not be purchased. Additionally, only two roaming nodes could be produced.

External Standards

The following external standards apply to this project.

1. *FCC Regulations* – The LoRa transceivers operate at 915MHz in the 902-928 MHz unlicensed band for ISM (industrial, science, and medical) applications. Thus, they are required to be type accepted for part 15 Federal Communications Commission (FCC) regulations. These modules are designed for wireless communication, so they are classified under Part 15 Subpart C as intentional radiators. Within this part, both sections §15.247 [13] and §15.249 [14] apply to this project.

§15.247 states the following for digitally modulated intentional radiators [13]:

1. The minimum 6 dB bandwidth of the signal shall be at least 500kHz
2. For digitally modulated systems, the power spectral density conducted from the intentional radiator to the antenna shall not be greater than 8 dBm in any 3 kHz band during any time interval of continuous transmission.
3. In any 100 kHz bandwidth outside the frequency band of operation the power shall be at least 20 dB below that in the 100 kHz bandwidth within the band that contains the highest level of the desired power.

§15.249 States the following for operation within the 908 - 928 MHz band [14]:

1. The maximum permitted field strength at a distance of 3m from the radiating source is 50mV/m

2. The maximum permitted field strength of harmonic components is 500μV/m at a distance of 3m from the radiating source

3. Emissions (other than harmonics) radiated outside of the 908 - 928 MHz band shall be attenuated by at least 50dB below the level of the fundamental.

The Semtech SX1262 transceiver is used for all LoRa communications. Thus, since it is FCC CFR Part 15 compliant, this project meets the necessary FCC regulations. Additionally, since the microcontroller operates at a frequency above 9kHz, it is regulated under the FCC's Part 15, Subpart B as an unintentional radiator.

The GPS receiver operates above the 960 MHz cutoff as described in FCC's Part 15.101, and thus are only to FCC's Part 15.5, which states that the device cannot cause interference and that it must accept any interference caused by a licensed radio station. The GPS receiver complies with these FCC regulations [15].

2. *NEMA Standards for Mechanical Casings* – The chassis is IP65 certified [16]. Thus, according to the National Electrical Manufacturers Association (NEMA), this means that the enclosure should be totally protected against dust ingress and protected against high pressure water jets from any direction [17].

3. *IPC Standards for PCB Design* – IPC standards determine many aspects of the PCB designs. IPC-2221A sets standards for the part and track spacings on the board designs [18], IPC-A-600F sets acceptance criteria for PCBs, including board edges, material,

holes, plating, solder mask, and much more [19] IPC-4101C sets standards for base materials for multilayer boards such as laminate and prepreg [20].

4. *SMD Component Packages* – SMT (surface mount technology) industry standards define standard sizes for SMD (surface mount device) components such as chip resistors, and small outline transistors (SOT). The leading standardization body is JEDEC [21]. This simplifies PCB design, as standard footprints are available in the Multisim master database and all standardized parts will fit those footprints. The boards use many industry standards including 0805 and 0402 rectangular passive components, a 20 lead 4x4 QFN (quad flat no-lead) voltage regulator, an 80-LQFP (low-profile quad flat-package) microcontroller, and an 8-SOIC hall effect current sensor, among others.

5. *USB (Universal Serial Bus)* - USB standards define communications between a computer and a peripheral device. They are developed and maintained by the USB Implementers Forum (USB-IF) [22]. A USB connection was used to relay data from the home node to the laptop that ran the user interface and to provide power to the home node.

6. *IEEE 1149.1 JTAG Standard* - The JTAG specification as defined under the IEEE 1149.1 standard is used for flashing and debugging the embedded code [23].

7. *UART (Universal Asynchronous Receiver-Transmitter)* - A UART is a block of circuitry responsible for implementing serial communication. UART transmits asynchronously between a transmitter and a receiver device [24]. UART requires a standard baud rate, which was set to 9600 bits/second, and was used to send data from the home node to a computer terminal.

8. *SPI (Serial Peripheral Interface) Communication Protocol* – SPI is a synchronous serial communication protocol for communication with peripheral devices in embedded systems [25]. SPI was used to communicate with the GPS module as well as the LoRa transceiver in separate peripherals. Each ran at 1 MHz clock speeds to conserve power.

9. *RoHS (Restriction of Hazardous Substances) Compliance* – RoHS is an EU standard that restricts the use of specific hazardous materials found in electrical and electronic products [26]. Most components used are RoHS compliant, which minimizes the environmental impact of the design.

Tools Employed

Several programming, design, and testing tools were used to complete this project. The tools for each distinct section of the project are described in detail below.

Hardware

To design and layout the boards, National Instruments' simulation and design tools Multisim [9] and Ultiboard [10] were used. These tools were necessary to create the board schematics, as well as to layout the boards. Although Jesse, who was the primary user of these tools, was familiar with both Multisim and Ultiboard from prior coursework, she had to improve her skills with both tools for the level of use this project required.

Firmware

The firmware was written in C using Texas Instruments' integrated development environment (IDE), Code Composer Studio [11]. The firmware for the project and for testing used several existing libraries, including the MSP430 driver library, *driverlib* [27], *stdint* [28], *stdio* [29], and

stdlib [30]. To load the code onto the boards and debug the firmware, the Texas Instruments' Flash Emulation Tool for MSP430 was used [31]. Finally, for testing and intermediary deliverables of the firmware, the terminal tool Tera Term was used [32].

Software

For the user interface (UI) of the system, Python 3.7 was installed using Anaconda Distribution [33]. The entire system was written in a simple text editor and run through the Anaconda terminal. The necessary Python packages were installed using Anaconda Cloud [34], and are the following:

- pyserial, to read data through UART
- folium, to load the map and plot the coordinates
- selenium, to load the Chrome page displaying the map
- pyautogui, to refresh the map display upon each new payload received

Demonstration

To implement the power system demonstration, National Instruments' design tool LabVIEW [35] and its embedded device myRIO [7] were used. These tools were necessary to acquire readings from the power system and visualize the power harvested and power consumed by a roaming node. However, both LabVIEW and the myRIO were new to several of the team members. Although Malcolm was familiar with both tools, Nojan, who collaborated with Malcolm on the power system demonstration, had to improve his skills in LabVIEW to help complete this portion of the project.

Ethical, Social, and Economic Concerns

Environmental Impact

Most of the electrical components are RoHS compliant, which minimizes their environmental impact. However, the materials used for the solar panels and the batteries are a large environmental concern. Solar panels, while a source of sustainable energy, are not recyclable, and their manufacturing processes involve toxic materials and a large amount of energy and water. Common problematic toxins in solar panels include lead, cadmium, and antimony [36]. Lithium ion batteries reduce the need for carbon-intense energy sources, but also involve toxic materials and have a limited lifetime. As few as 5% of lithium ion batteries are recycled, and the main ingredients such as cobalt and lithium are exhaustible resources whose extraction can lead to water pollution, environmental degradation, and inhumane working conditions [37]. Cobalt mines exploit workers through meager wages, child labor, and unsafe working conditions [38].

Sustainability

This project presents a more sustainable design than prior work by implementing a self-powered system designed for durability and long lifetime. However, the lifetime is not infinite. Lithium ion batteries have about a two to three-year lifetime, and solar panels degrade year by year, with a final lifetime of about 25 years [36]. The batteries will therefore limit the lifespan of this fleet tracker, but the power system is modular and batteries can be replaced without affecting the rest of the system. Batteries will also affect the scalability of the system. As electric vehicles grow in popularity, the demand for lithium ion batteries will increase which raises the price. Analysts estimate an eleven-fold increase in demand for cobalt due to lithium ion batteries by 2025 [39]. Supplies of lithium are running out, which will affect the future availability of our batteries.

However, as battery recycling becomes more economically viable, greater supplies of lithium will be available [39].

In addition to batteries, the range affects the scalability of the system. Currently, the transceivers have a range of approximately 0.25 miles, and without infrastructure existing to link nodes together, the system is confined to that range. Stronger antennas and a larger power system may increase that range. An infrastructure network of stationary home nodes would be necessary to transfer the data across long distances and properly scale the system. Additionally, while the system will enact protections against data collisions, adding many more roaming nodes may lead to complications.

Health and Safety

The main safety concern in this system are the lithium ion batteries. They pose a risk of fire or explosion if handled incorrectly, which could lead to personal injury, property damage, or even death [40]. The boards are made of FR-4 material, which is flame retardant, nevertheless considerable care must be taken when handling the batteries. The boards have proper battery protection circuitry, which reduces the risk of battery malfunction. However, it is necessary for users and manufacturers alike to be aware of the potential risks that the batteries pose.

Manufacturability

The GPS tracking system will be relatively simple to reproduce, especially at large scales where surface mount technology (SMT) can be used to populate the boards. The PCBs are the only components that require custom manufacturing, as the enclosure, solar panel, and batteries are standard components available from manufacturers. All PCB components are inexpensive and discounts are available with increased quantities. The main limitation to increased production is

the GPS breakout board, which is available from SparkFun and on Digikey for approximately $45. However, as of December 2019, the quantities are limited (52 in stock on SparkFun [41], and 49 from Digikey [42] and would therefore limit the number of boards we could produce.

To build the project, the main required skill is soldering. The boards contain both surface mount and through hole components and many of our packages are rather small (0402) and fine-pitch. This means that somewhat advanced soldering skills are necessary. However, once the system reaches scales where SMT is feasible, that will no longer be an issue. Additionally, once the board is soldered, it needs to be programmed. On a large scale, this could be automated by having a designated file that would be loaded onto all boards with a modifiable portion that assigns a unique ID to each roaming node. After the board is programmed, it needs to be tested. This requires checking electrical connections and supply voltages as well as testing the RF section which would require knowledge of a spectrum analyzer.

Ethical Issues

As the proposed project is a fleet tracker, scalability is integral to the success of the product. The system should always keep data secure, whether 2 or 2,000 nodes are being used. An attempt at ensuring data privacy was using a secure, computation-light form of AES encryption. The use of encryption gives the product the ability to scale. One of the biggest security risks in scaling the IoT is packet-sniffing, which is when a bad actor in the network intercepts a packet that is being sent between nodes and reads the data within it [43]. As the system is handling location data, which is very important to keep secure, future iterations of the system should keep this data as inaccessible as possible to packet sniffers while still meeting the

power budget. As more and more nodes are being added to the network, the points of attack for packet-sniffers increases, which is why scaling up IoT networks can be dangerous.

The form of encryption that was attempted in implementation encrypts the data on the roaming node upon transmission, using a key that only the home node has to decrypt the data. This form of encryption can be made very energy-efficient for the roaming node and helps avoid packet-sniffers accessing user's location data. The system demonstrated at the Capstone Fair did not have encryption successfully implemented, although all of the code was written and worked on different data. When the encryption is run on the packet that is being transmitted from the roaming node, the device ID was also encrypted, which is required for the LoRa transmission. This problem was not overcome before the Capstone Fair, and encryption has been listed as one of the "Future Works" for this project.

Intellectual Property Issues

[44] presents a patent for a "Vehicle information system". The technology presented is classified as "Registering or indicating the working of vehicles communicating information to a remotely located station". This patent's main independent claim is "one or more communication protocols configured for communication between at least one of: the [On Board Diagnostics (OBD)] interface device and a client electronic device, the OBD interface device and a server computer, and the OBD interface device and a wireless receiver; and an application programming interface configured to allow interaction between the OBD interface device and at least one of: a server computer and a client electronic device." This is backed up by a dependent claim that "the vehicle fleet tracking features include providing one or more of: vehicle location, fuel consumption, speed, location history, duration of trip, VIN, year, make, and model." In light of

these claims, the capstone that is presented is still patentable, as the system developed by Dugan's Dogs has installation that does not rely on an OBD interface, only communicates with LoRa, and does not run off the car battery. The other independent claims focus in on the different aspects of the system, such as the communication protocol and OBD connection.

[45] presents a patent for a "Satellite-positioning-system tracking device and method for determining a position of the same". The technology presented is classified as "Interaction or communication between different cooperating elements or between cooperating elements and receivers providing aiding information employing an initial estimate of the location of the receiver as aiding data or in generating aiding data". This patent is described as "global navigation satellite system-tracking ("GNSS-tracking") device and method for determining one or more positions of the GNSS-tracking device utilizing a user-plane service." The two main independent claims are "tracking circuitry for determining at least one position of the tracking module using the user-plane service in a satellite positioning system" and "a chargeable source for supplying power to the tracking circuitry when disengaged from the charging module, and wherein the charging module is operable to charge the chargeable source when the charging module is coupled to the tracking module." Backing up the second claim is a dependent claim stating "charging module comprises circuitry for converting energy received from at least one external source into power for charging the chargeable source." Although this would mean that our solar charging falls under these claims, this system uses cellular networks to communicate and two receivers within the system, which are features that are listed under independent claims. The team's presented capstone only uses one GPS receiver and communicates via LoRa, so the capstone remains patentable.

Finally, [46] presents “Safety status sensing system and safety status sensing method thereof”. The technology presented is classified as “Communication between parent and child units via remote transmission means, e.g. satellite network”. This patent’s main independent claim is “A safety status sensing method for a safety status sensing system, the safety status sensing system comprising a LoRa host, a first wearable sensing device and a second wearable sensing device, and the LoRa host communicating with the first wearable sensing device and the second wearable sensing device according to a LoRa protocol.” One of the dependent claims states that “the first wearable sensing device has a first device ID, and the first device LoRa protocol transceiver is further configured to receive a host GPS location from the LoRa host”. Essentially, this is a safety wearable that transmits GPS location between wearables using LoRa communication. The power supply and charging methods are not mentioned as dependent or independent claims. This patent is limited to wearables using GPS and LoRa to communicate with each other, while the presented capstone can be used within a range of applications. The presented capstone also utilizes solar power to charge a battery to power the system. In light of the claims made by this patent and the aforementioned patents, Dugan’s Dogs’ Fleet Tracker is patentable.

Detailed Technical Description of Project

The goal of our project was to develop a self-powered GPS tracking system that communicates using LoRa transceivers as a proof of concept for IoT applications in rural areas. The system has been broken down into the following sections:

1. Hardware
    i. Roaming Node Power System
    ii. Schematics
        1. Home Node
        2. Roaming Node
    iii. PCB design
        1. Home Node
        2. Roaming Node
2. Firmware
    i. General Firmware
    ii. GPS
    iii. LoRa Transceiver
    iv. Reliable Data Transfer Protocol
    v. Media Access Control Protocol

3. Software User Interface

4. Mechanical Casing

A high-level system block diagram is shown in Figure 1.

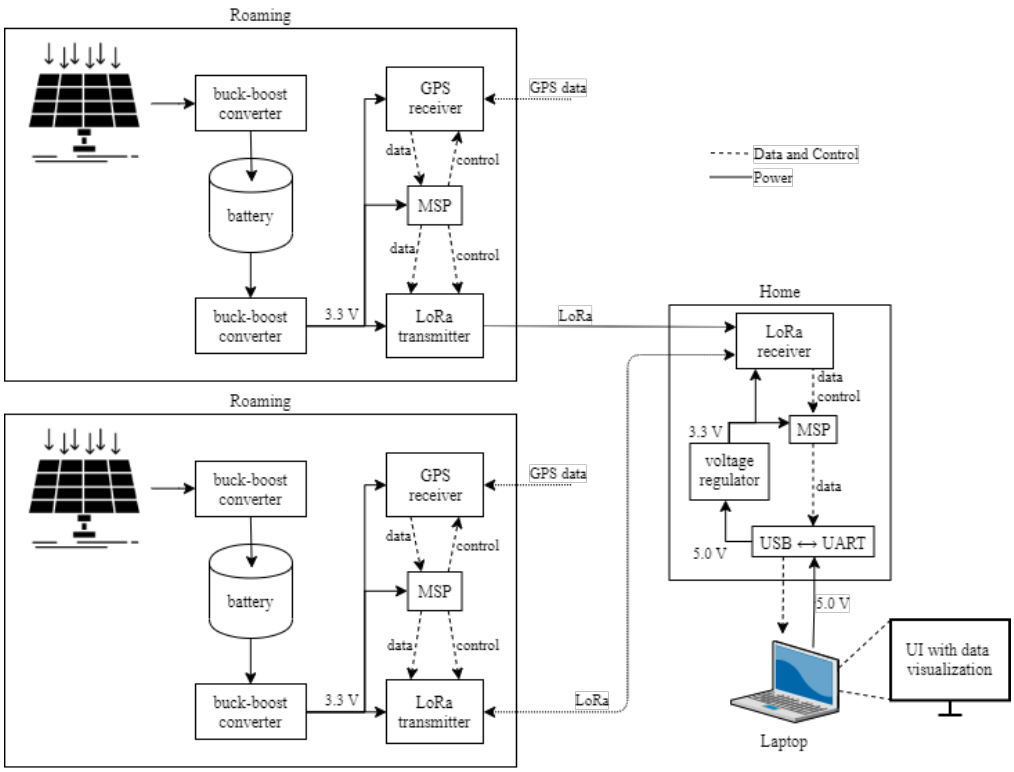

Figure 1. System Block Diagram.

Hardware

The hardware consists of one central home node and two roaming nodes. The home node is powered through USB and contains a LoRa transceiver, an MSP430 microcontroller, and a USB to UART interface board. The roaming node is self-powered through a solar panel and a lithium-ion battery, and contains a GPS receiver, a LoRa transceiver, and an MSP430 microcontroller. The development of these modules is described in the following sections.

Roaming Node Power System

The overall goal of the power system was to provide consistent power to the roaming node for as long as possible. To do this, the power system was designed with the following goals:

1. Harvest as much energy as possible
2. Be able to store as much energy as possible
3. Consume as little energy as possible

A major constraint with this goal is the physical size of the final product. To maintain compatibility across many different vehicles, the device must be relatively small. To accomplish goal 1, a monocrystalline solar panel was selected with a maximum power output of 2.5W. For energy storage, we selected an 18650 lithium-ion battery. This series of lithium ion cell offers high energy density, which satisfies goal 2. The solar panel was paired with an IC [47] that was specifically designed for charging lithium ion batteries from solar panels. Finally, to use as little power as possible, the microcontroller, GPS, and LoRa transceivers were configured to operate in the lowest functional power modes.

To test the power system, models for the energy production, storage, and consumption of the roaming node were created.

In terms of energy harvesting, the solar panel is rated for 2.5W in full sunlight. Even in poor lighting, solar panels can output about $10 - 25\%$ of their maximum power [48]. At latitude 40°N, the shortest day of the year is just over 9 hours long [49]. This means that the lowest amount of energy that could be harvested from a roaming node's solar panel in one day with these conditions is $0.1 * 2.5 * 9 = \mathbf{2.25Wh}$.

The lithium ion battery has an initial rated discharge capacity ≥ 3,350mAh. After 500 cycles, the capacity is rated at ≥ 2,010mAh. Since this device is intended for long term use, 2,010mAh will be used as the capacity for the following calculations. To obtain the energy capacity of the cell, the capacity in mAh was multiplied by the nominal voltage of the cell, 3.7V [50]. Thus, for the following calculations, the energy capacity of the battery will be treated as 2,010mAh∗ 3.7V = **7,437mWh**.

The three main sources of power draw in the roaming node system are the microcontroller, the GPS module and the LoRa transceiver. A 3.3V supply voltage is sued for the entire board.

With a $\frac{1}{15} \approx 0.67$Hz duty cycle, the LoRa transceiver is expected to draw an average current of approximately 5mA (See Appendix A). In active mode at 1MHz, the microcontroller draws 470uA [51]. In power save mode (1Hz data acquisition rate), the GPS module's typical current draw is 8.5mA. At output currents between 10mA and 200mA, the buck-boost converter has a rated efficiency 90% [52]. Thus, the overall average current draw is estimated to be approximately $\frac{1}{0.9}(5mA + 470uA + 8.5mA) \approx 15.5mA$. With the supply voltage of 3.3V, the roaming node will draw an estimated $3.3V * 15.5mA * 24hours \approx \mathbf{1.23Wh/day}$.

Schematics

The schematics for both boards were developed in NI Multisim and are described below. Schematic design began by prototyping using an MSP430F5529 Launchpad [51], a LoRa transceiver evaluation board [54], and a GPS breakout board [41]. The MSP430F5529 was chosen for its multiple GPIO pins, internal flash memory, and multiple SPI lines. However,

many other models of the MPS would have worked fine, and the MSP430F5529 has 80 pins, which complicated the footprint, schematic, and soldering process. The SX1262 LoRa transceiver was chosen because Jesse and Vivian had prior experience working with it during their summer internship and had already developed basic embedded code for the device. It has the best receiver sensitivity and power output of available LoRa transceivers. Additionally, one of its suggested applications is asset tracking (https://www.semtech.com/products/wireless-rf/lora-transceivers/sx1262). Finally, the SparkFun GPS Breakout – ZOE-M8Q board was chosen as the GPS module because of its small form factor and relatively low price. These boards were connected via jumper wires to form prototypes, which were used to verify the design and to develop schematics for the home and roaming nodes.

Home Node

The home node contains three functional blocks, shown in Figure 2. Its purpose is to receive GPS tracking data from each roaming node and to transmit that to a laptop, where the tracking data is displayed on a map.

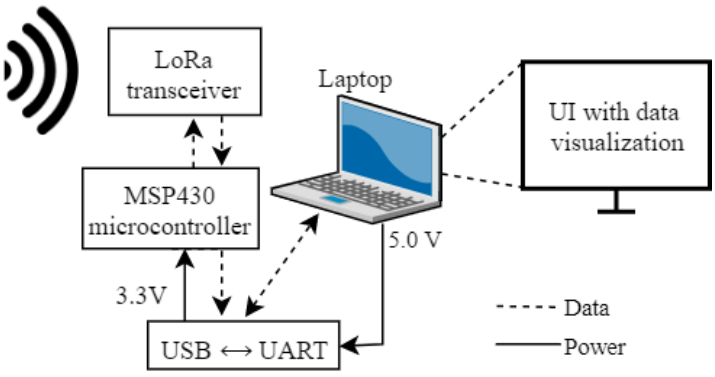

Figure 2. Home Node System Diagram.

The home node schematic incorporates all functional elements of the prototype. This includes components from the MSP launchpad and the LoRa evaluation board. The launchpad consists of three sections: the microcontroller, a USB hub including a voltage regulator and a USB to UART device, and a JTAG debugging section. All of these sections were incorporated into the home node. The FTDI UMFT234XF USB to UART board [54] was used in place of the UART device on the launchpad, and contains a voltage regulator, so 3.3V power was sourced from that board to the rest of the home node. A JTAG header was included to allow for simple, on-board programming. The reference schematic on page 21 of the MSP430 Hardware Tools User's Guide [55] was used for the JTAG connections. The schematic for the MSP launchpad was used to determine the appropriate components needed to mimic the launchpad design [56]. This included bypass capacitors and pull-up/pull-down resistors. The LoRa evaluation board included a transceiver, impedance matching filters, and an RF switch, and all were incorporated into the home node using the reference design files found on Semtech's website [57]. To preserve the functionality of the prototype, that section was copied exactly from the evaluation board, including component values and footprints. The final home node schematic is shown in Figure 3. Debug components include LEDs and test pins. The home nodes were designed before the roaming nodes, so GPS connections were included for testing. A full bill of materials (BOM) for the home node can be found in Appendix C.

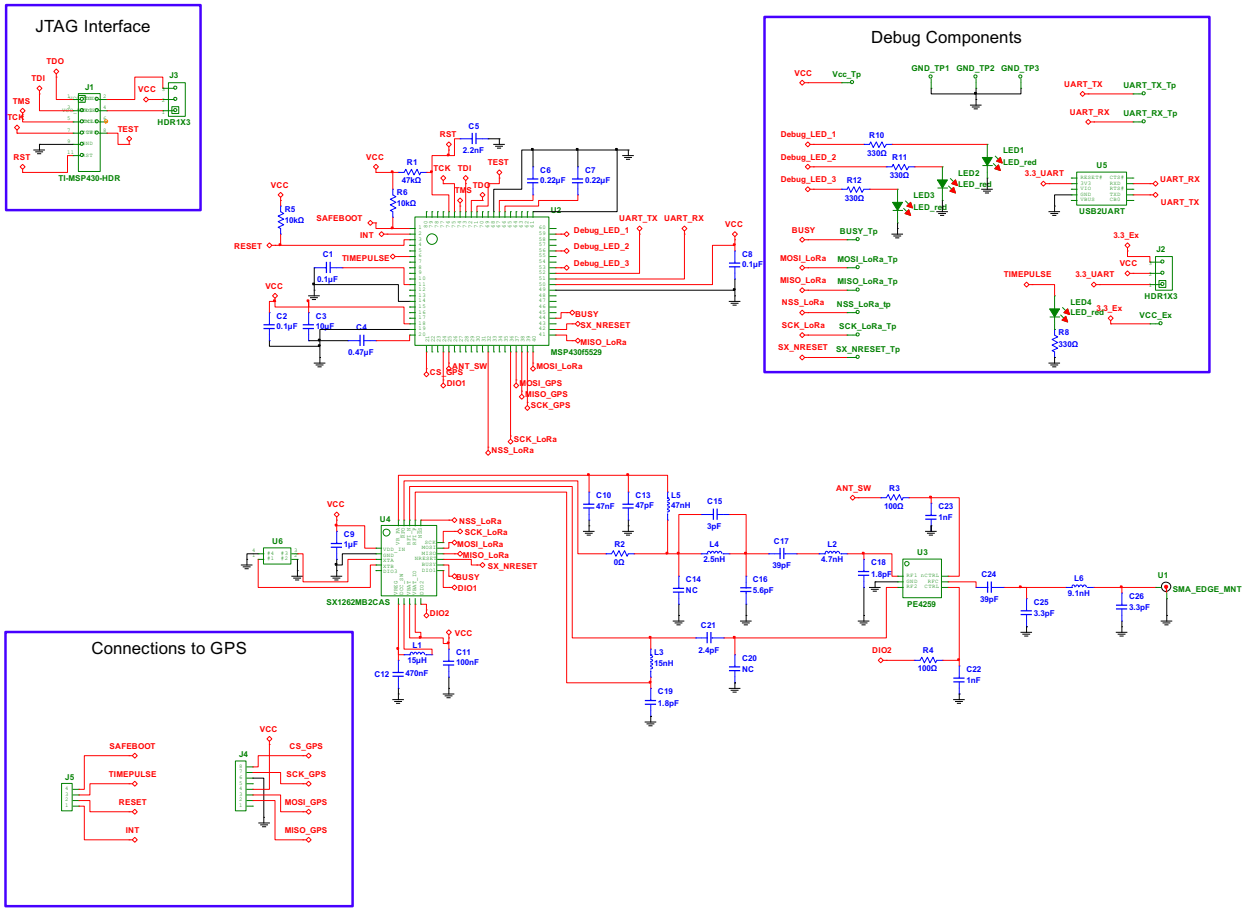

Figure 3: Home Node Schematic

The RF subsystem can be seen in Figure 4, and includes the transceiver, 50-ohm impedance matching filters, and an RF switch, all copied exactly from the evaluation board since no team member has experience in RF circuit design or impedance matching filter design.

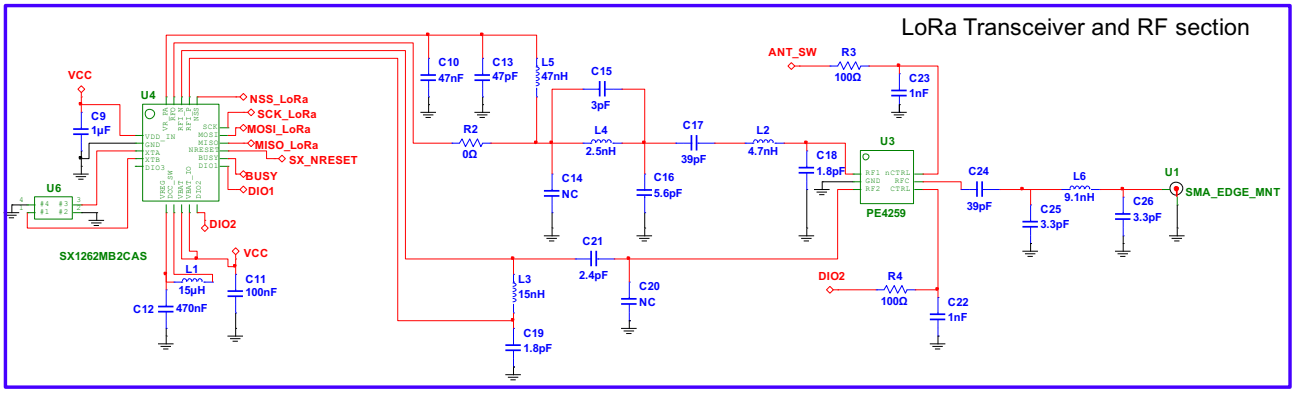

Figure 4: RF Subsystem Schematic

Roaming Node

Each roaming node contains six functional blocks, three for the power system, and three for the communications. These are shown in Figure 5.

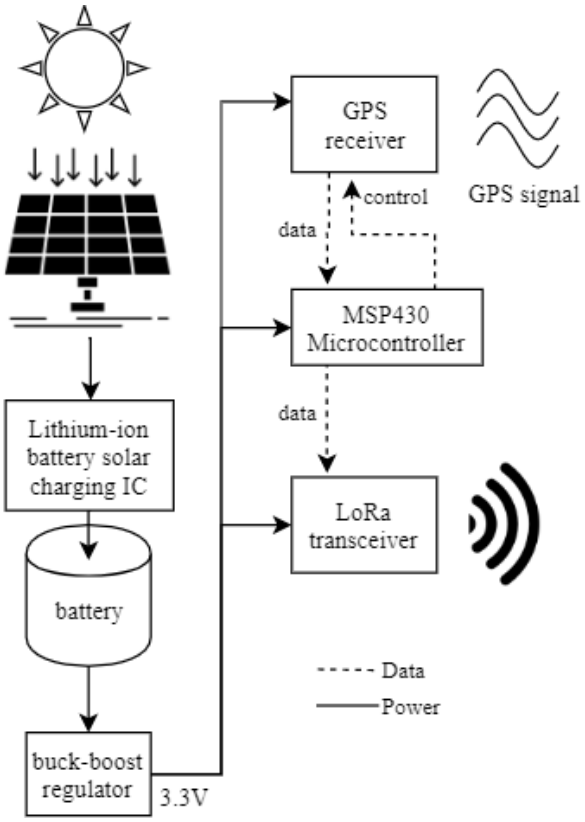

Figure 5. Roaming Node System Diagram.

The power system includes a solar panel input, the BQ24210 lithium-ion battery solar charger [47], a Samsung 18650 lithium-ion battery [50], and an ISL91127IR 3.3V fixed-output buck-boost voltage regulator [58]. The battery charging IC was specially made for lithium-ion batteries, and supplies a maximum of 800mA when charging. This is ideal for our design, as it can supply the maximum power from our solar panel to the battery. The buck-boost converter

was chosen for its high output current (up to 2A) and its footprint, as the QFN package was one of the largest and easiest for WWW Electronics to solder compared to the other potential regulators. In addition to those essential parts, two current sensor ICs were included to monitor the current entering and leaving the battery. These were used to verify the power system.

Besides the power system, the roaming node schematic is the same as the home node schematic save for a few minor additions. More header pins were added for debugging and a myRIO connection was used to verify the power system. The roaming nodes both also include the FTDI UMFT234XF USB to UART board as an alternate power supply and for easy debugging using a terminal emulator such as TeraTerm. A full BOM can be found in Appendix C.

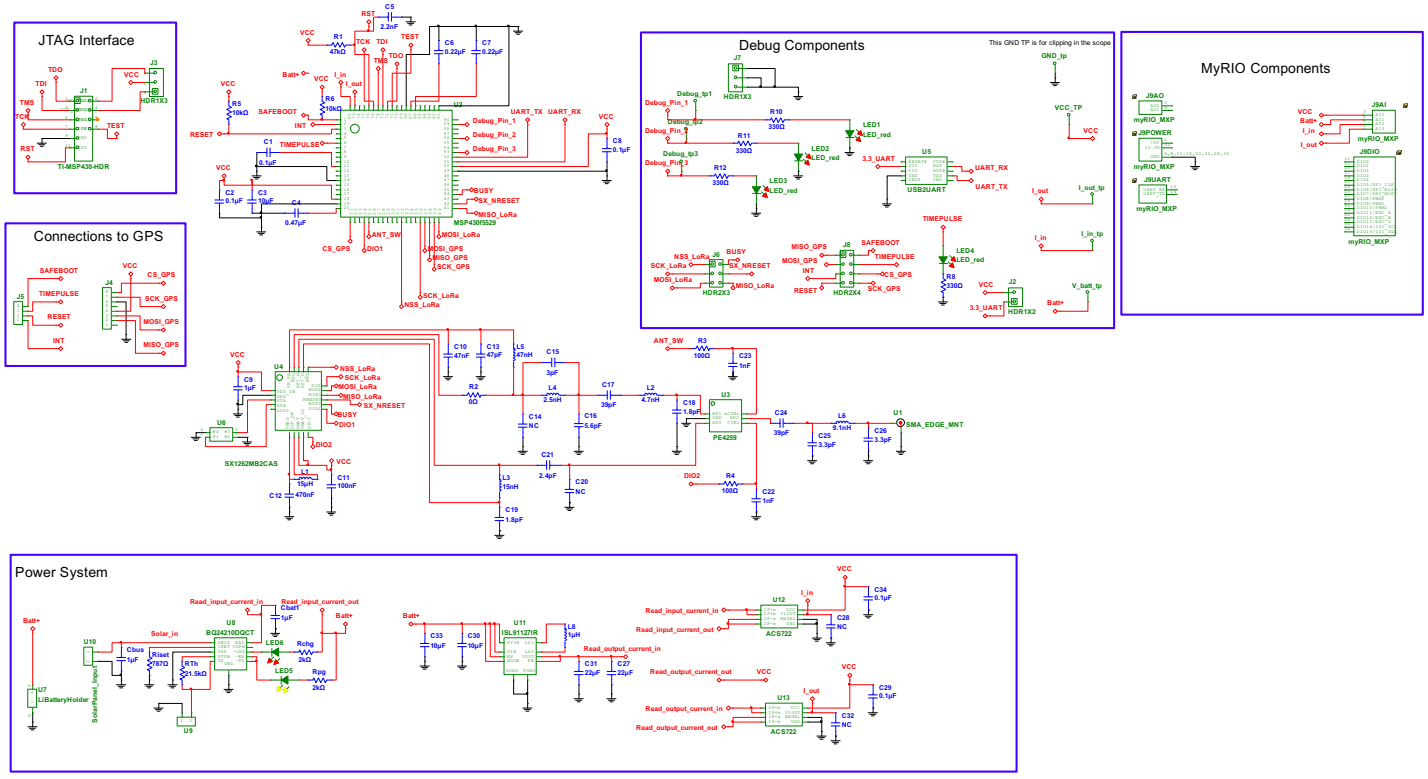

Figure 6: Roaming Node Schematic

The power subsystem schematic is shown in Figure 7. All external components for the ICs were taken directly from the respective datasheet to minimize errors. The current sensors were connected in series with the battery input and the output from the buck-boost regulator.

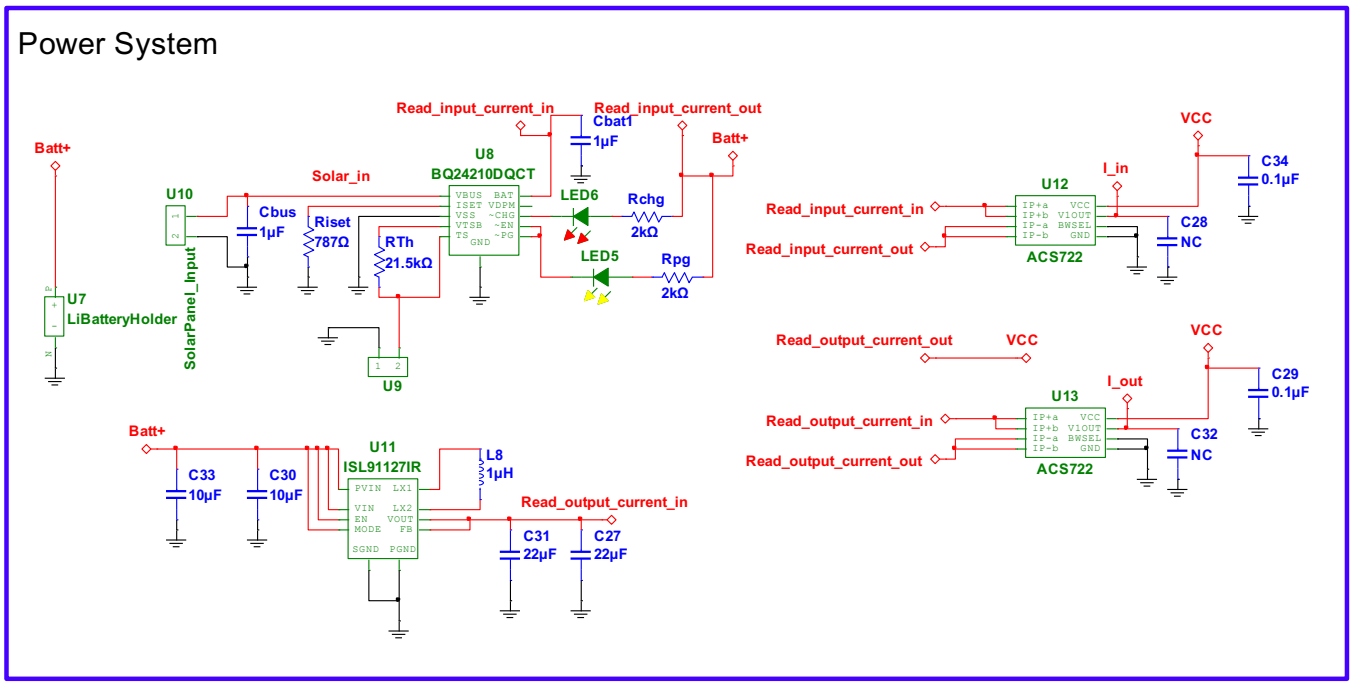

Figure 7: Power Subsystem Schematic

PCB Design

The PCB design for both boards was done in NI Ultiboard. Both the home and roaming node are a four-layer FR4 board. This was done to mimic the design of the LoRa evaluation board to maintain the RF performance. The top layer contains all components and the traces for the RF section and the input power as well as some SPI connections between the microcontroller and peripheral devices (LoRa and GPS). The second layer is a ground plane which forms a coplanar waveguide in the RF section between the transceiver and the antenna. The third layer is

a power plane, providing 3.3 V to all devices. The bottom layer contains traces that were difficult to route on the top layer.

The Semtech SX1262 evaluation board [53] was used as a reference design for the layout of the RF section of both nodes. CAD project files, as well as a bill of materials [57] and design explanation [59] for the evaluation board reference design, are available from Semtech's website. The bill of materials was used to determine component values that are missing from the schematic.

The layout and components of the RF section were copied exactly from the Semtech reference design including DNC capacitors and jumpers for the RF section of the home node and the roaming node design. As in the reference design, the DC-DC configuration was used to minimize power consumption, and the crystal oscillator was thermally isolated to reduce frequency drift. Impedance matching filters reduce loss between the transceiver and the antenna. The values for these filters are explained in the reference design explanation and were not changed from the reference design. The trace thickness and component spacing for the RF section were originally mimicked on the home and roaming nodes, then adjusted to meet manufacturing needs. The antenna for the LoRa communication is the same as the antenna provided with the reference board.

To comply with Advanced Circuit's student special for 4-layer boards, the boards had to be a standard thickness of 62 mil. The reference board is not a standard thickness, it is 1 mm (39.6 mil) thick. However, all 4-layer advanced circuits boards must be 62 mil thick, with an inner core of 39 mils and a dielectric thickness of 9.3 mil [60]. To adapt the design to this new board thickness, the coplanar waveguide section had to be modified to reflect the increased dielectric

thickness of 9.3 mil vs 5.906 mil. These modifications included redefining the areas without copper around the traces, as well as the trace thicknesses. The copper around each trace should back off the same distance as the dielectric thickness, and an impedance calculator was used to determine that each trace should be increased to 16 mils to maintain the proper impedance on each line. A screenshot of that calculation is shown in Figure 8. The final coplanar waveguide set-up can be seen in Figure 9, and includes the proper trace thickness, dielectric thickness and ground plane spacing.

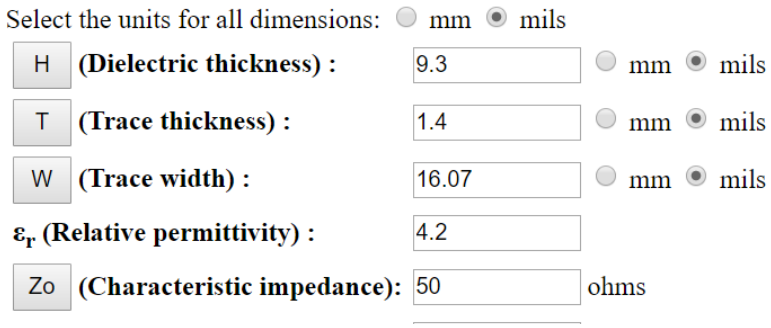

Figure 8: Impedance Calculator to Determine Trace Thickness for RF Section [61]

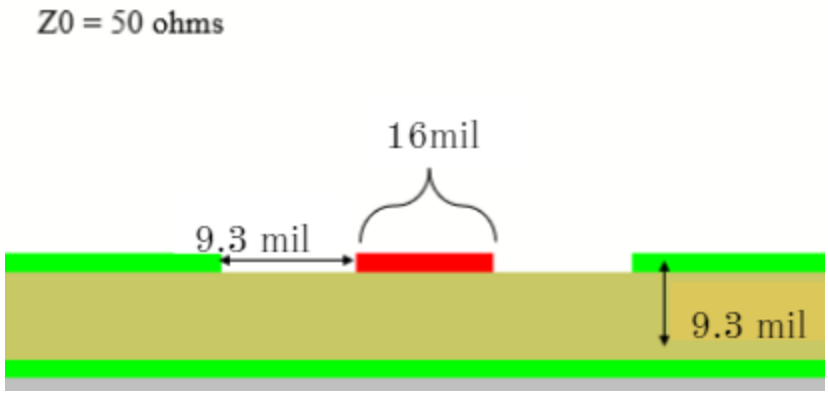

Figure 9: Coplanar Waveguide

The home and roaming nodes both utilize fencing and stitching vias. Fencing vias line RF traces, and at for 915 MHz should be no more than 100mils apart. Stitching vias aid in thermal dissipation and noise reduction and were placed across the RF section. However, Advanced Circuits requires fewer than 50 vias per square inch of board, which limited the number of stitching vias used in comparison to the reference design.

The layout for the rest of both boards was chosen to minimize board size and routing complexity. Traces not in the RF section are 10mil thick, which are more than enough to carry the required current since the board is low-power (<500mA). Boards were populated at WWW Electronics, Inc. (3W) and by hand by the team. 3W soldered the fine pitch ICs and the 0402 components, while the team hand soldered the 0805 components, headers, test pins, and connectors.

Home Node

Figure 10 shows the final board layout for the home node with the top ground plane hidden for clarity, and Figure 11 shows the final board with all power planes visible. Figure 12 gives a closer look at the RF section layout and routing in both 2D and 3D. The home node allows for power to be provided by a USB connection or via an external power source. Attaching a jumper between VCC_UART and VCC selects USB power, and a jumper between VCC_EX and VCC selects an external source that is connected to the VCC_EX test pin.

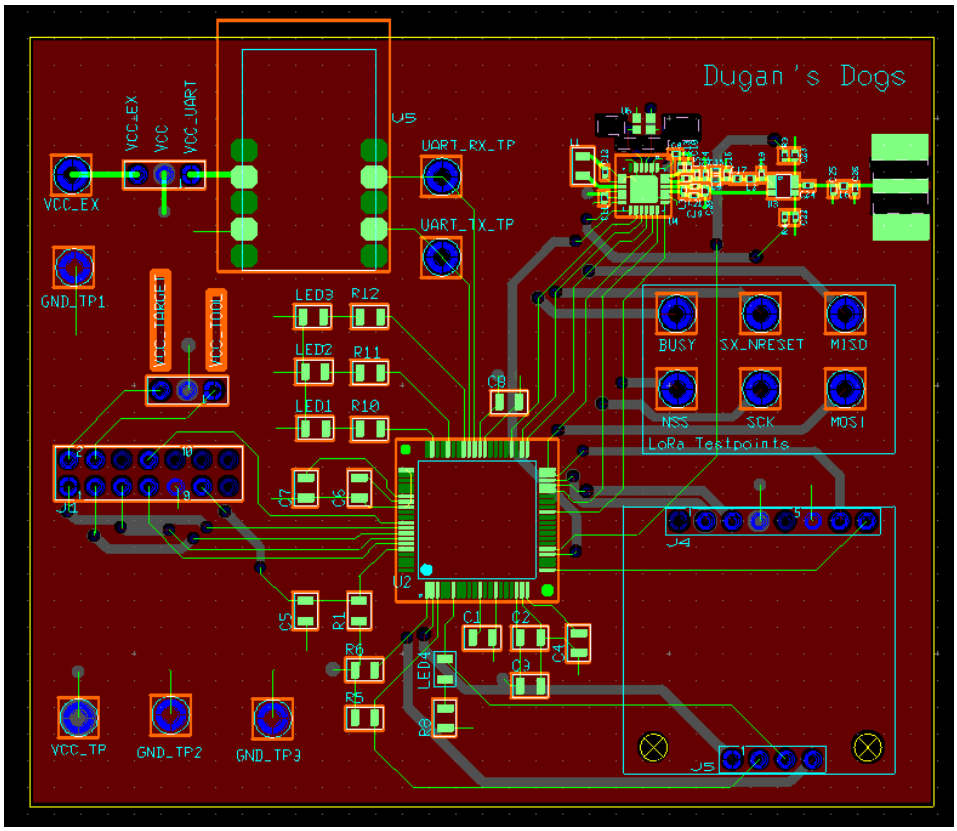

Figure 10: Home Node Layout and Routing (Top Layer Ground Plane Hidden)

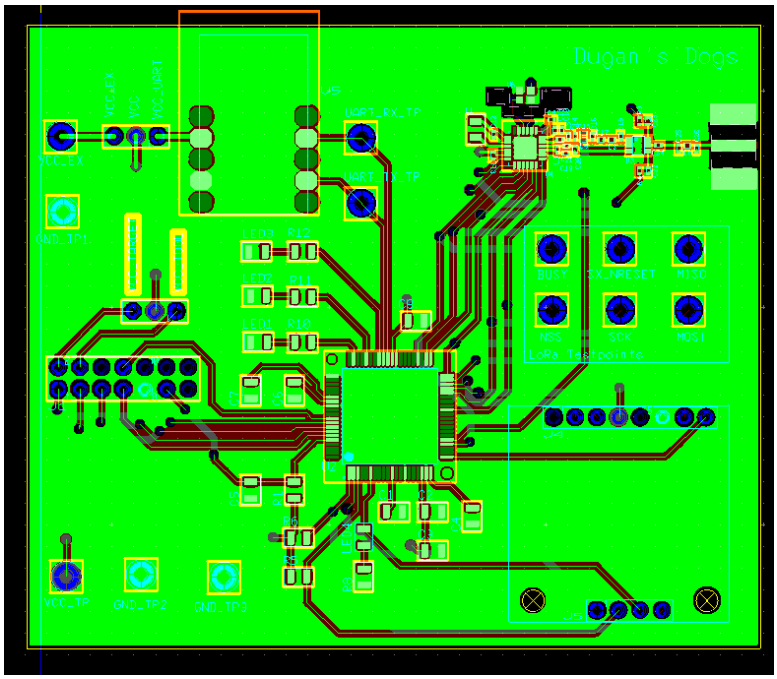

Figure 11: Home Node PCB Design

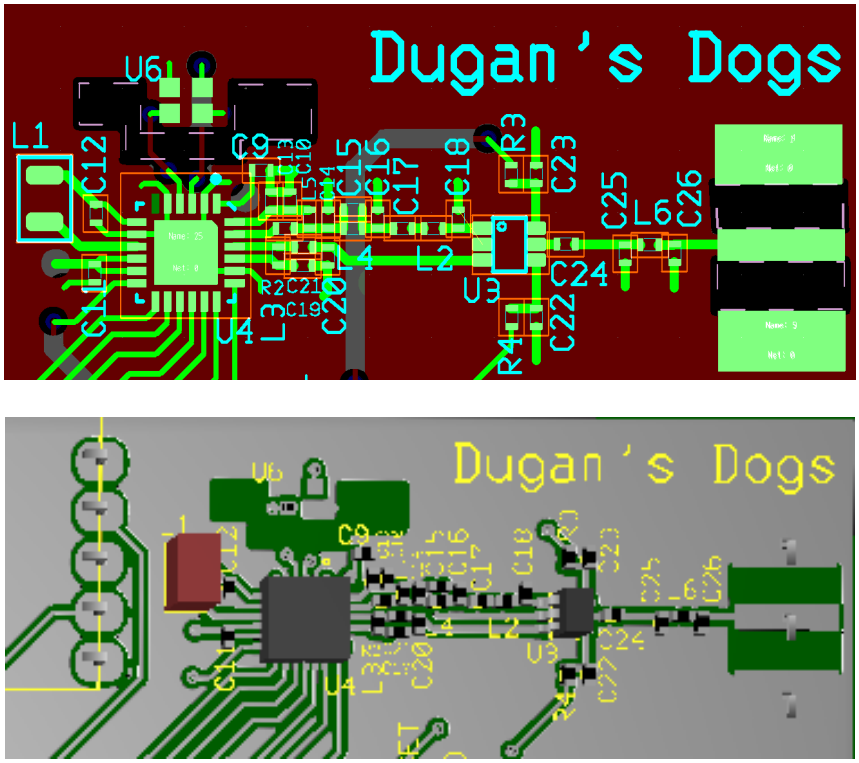

Figure 12: RF Subsystem Layout and Routing (Top: 2D view, Bottom: 3D view)

Roaming Node

Figure 13 shows the final board layout for the roaming node with the top ground plane hidden for clarity, and Figure 14 shows the final board with all power planes visible. The RF section is the same as the home node and can be seen in Figure 12.

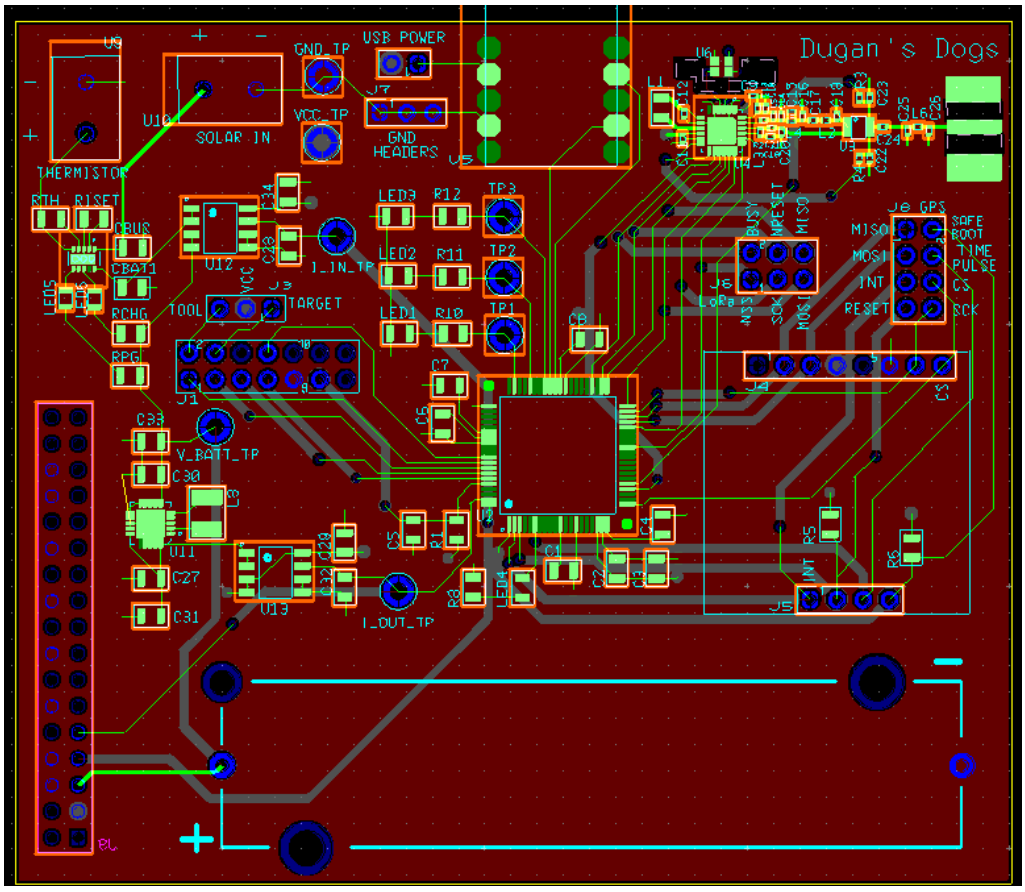

Figure 13: Roaming Node Layout and Routing (Top Layer Ground Plane Hidden)

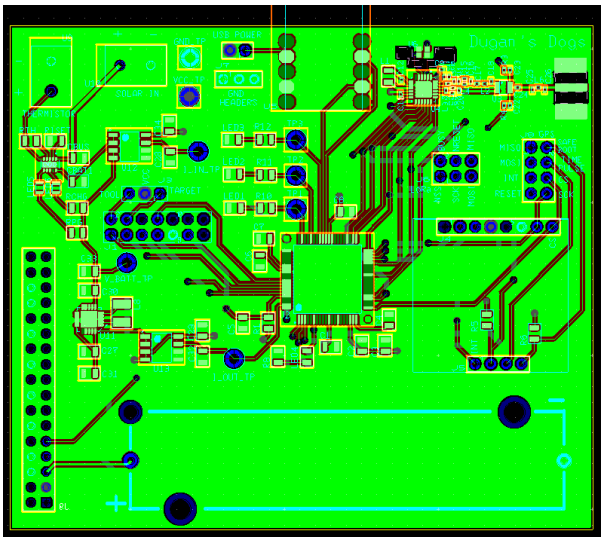

Figure 14: Roaming Node PCB Design

The roaming node allows for power via a USB connection for debugging or via the power system described in the Roaming Node Power System Section. Attaching a jumper between the USB Power pins pulls 3.3V directly from the USB to UART interface board, and disconnecting the jumper selects the power system power. To use USB power the battery and solar panel must be disconnected, and to use the self-powered system at least the battery must be connected. The GPS breakout board attaches as a header board to pins J4 and J5. This was done because 3W could not solder the GPS module directly onto the board as it is a ball grid array (BGA) component. The GPS antenna attaches to the breakout board. The myRIO connector was placed on the bottom of the board for easier connection. The unpopulated and populated boards for one roaming node are shown in Figure 15.

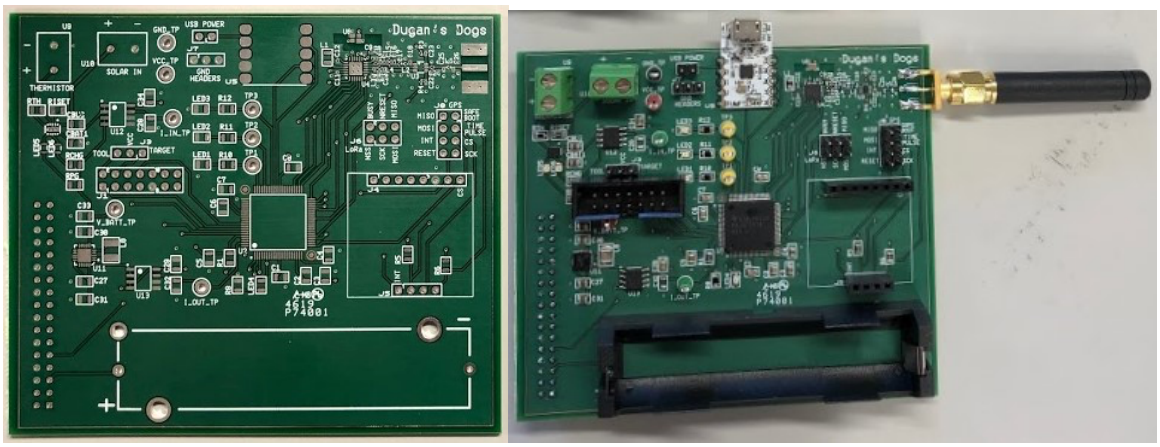

Figure 15: Left: Unpopulated Roaming Node, Right: Populated Roaming Node

Firmware

General Firmware

The firmware flow for the roaming node is represented in Figure 16, which shows the high-level flow on the left and detailed sub-blocks on the right. The firmware flow for the home node is represented in Figure 17.

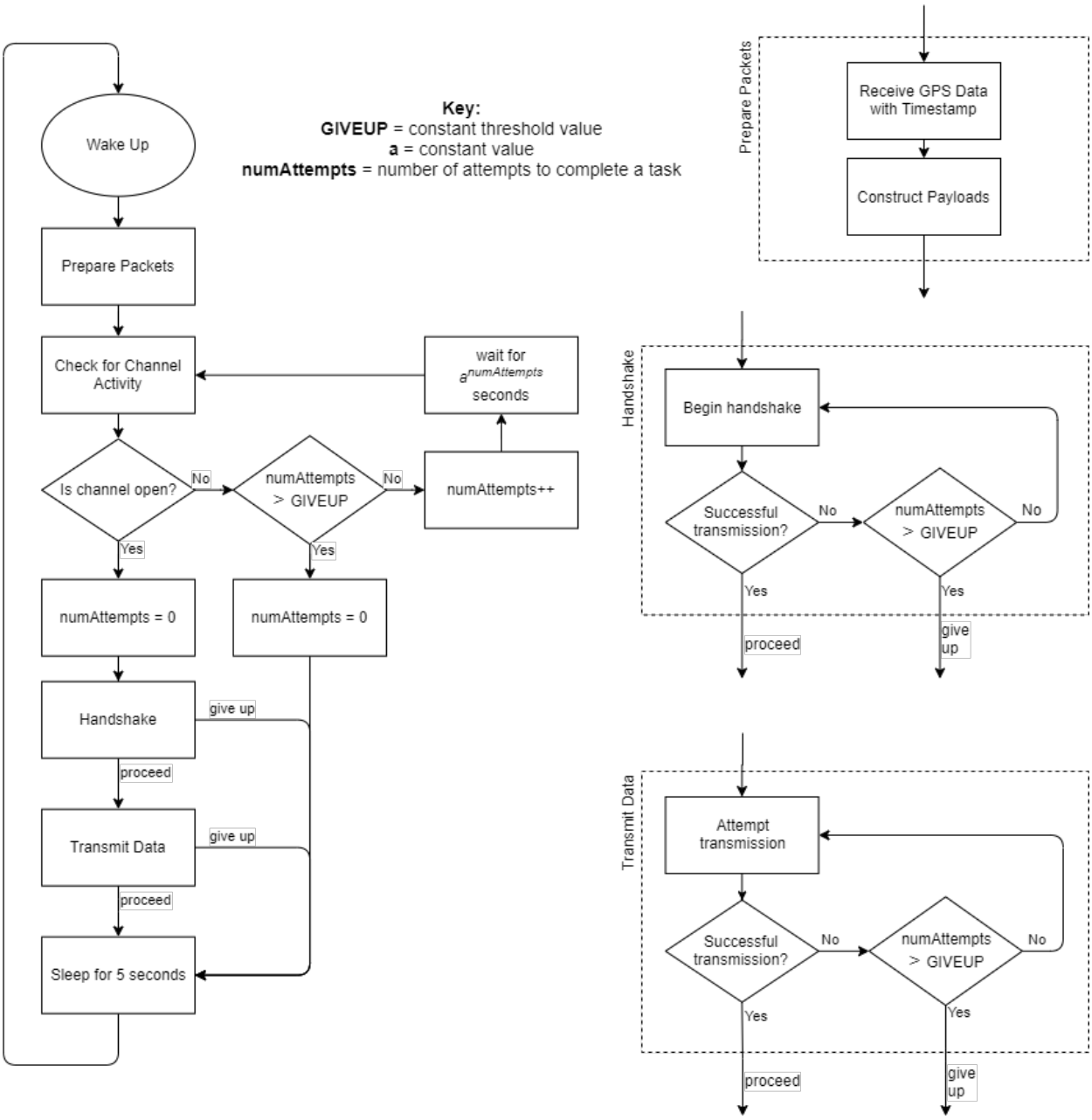

Figure 16: Roaming Node Firmware Flow Diagram, with *GIVEUP* = 4 and *a* = 2.

The roaming node operates in an infinite loop, beginning with a wake-up sequence. It then reads data from the GPS, which includes location coordinates and a timestamp. This data forms the payload for a single packet, which the roaming node will then attempt to transmit to the home node. For more information about the packet and payload, see the Detailed Technical

Description: Firmware: LoRa Protocol section of this report. Further details for the GPS data can be found in the Detailed Technical Description: Firmware: GPS section of this report. To transmit this data, the roaming node executes a series of protocol-related tasks.

First, to reduce the probability of a data collision with another transmitting node, the roaming node follows a media access protocol (MAC). In accordance with the Carrier Sense Multiple Access (CSMA) with Collision Avoidance (CA) protocol, the roaming node senses the communication channel for activity and, if none is detected, transmits the packet [62]. The Fleet Tracker implements CSMA-CA with exponential back-off. That is, if activity is detected, then the node waits for an exponentially increasing amount of time before sensing the channel again. This exponential back-off implementation uses a base of 2, meaning each successive failure will result in a wait time of 2 seconds, 4 seconds, 8 seconds, etc. For more information about MAC protocol, see the Detailed Technical Description: Firmware: Media Access Control Protocol section of this report.

Second, to establish a connection with the home node, the roaming node follows a reliable data transport (RDT) protocol. The RDT procedures begin with a handshake, in which the roaming node sends the home node relevant information about the data transfer to follow. Upon a successful handshake, the roaming node begins the data transfer. During the data transfer, the RDT ensures that packet errors and packet retransmissions are handled appropriately, such that the receiving node only receives and processes correct data. For more information about the RDT protocol, see the Detailed Technical Description: Firmware: Reliable Data Transport Protocol section of this report.

Upon a successful data transfer, the roaming node sleeps for five seconds, following a basic duty-cycling scheme. In this sleep mode, the MSP430 enters one of six possible low-power modes. The Fleet Tracker currently uses low-power mode 1 (LPM1), which disables the central processing unit and the frequency-locked loop. However, LPM1 allows the microcontroller's auxiliary clock (ACLK), sub-system master clock (SMCLK), and GPIO pins to remain active. This mode was chosen because, with an active SMCLK, the microcontroller in sleep would not affect the peripheral devices, such as the GPS module and the LoRa transceiver. The low-power modes can be found in the MSP430F5529 data sheet, on page 52 [51]. To enter a sleep mode, a number of control bits are set in the MSP430's status register. The control bits, and sample code for entering and exiting low-power modes can be found in the MSP430F5529 user guide, in pages 65-67 [55].

At each step in the protocol procedure, the roaming node has an opportunity to "give up" on transmitting the current data. This opportunity occurs during channel sensing, the handshake, and the data transfer. After a specific number of failed attempts, labeled *GIVEUP* in the roaming node flow diagram, the roaming node will skip the remaining data transmission tasks. It will immediately enter sleep mode for five seconds, then wake up and repeat the process with a new set of data. This implementation of the Fleet Tracker uses a *GIVEUP* value of 4.

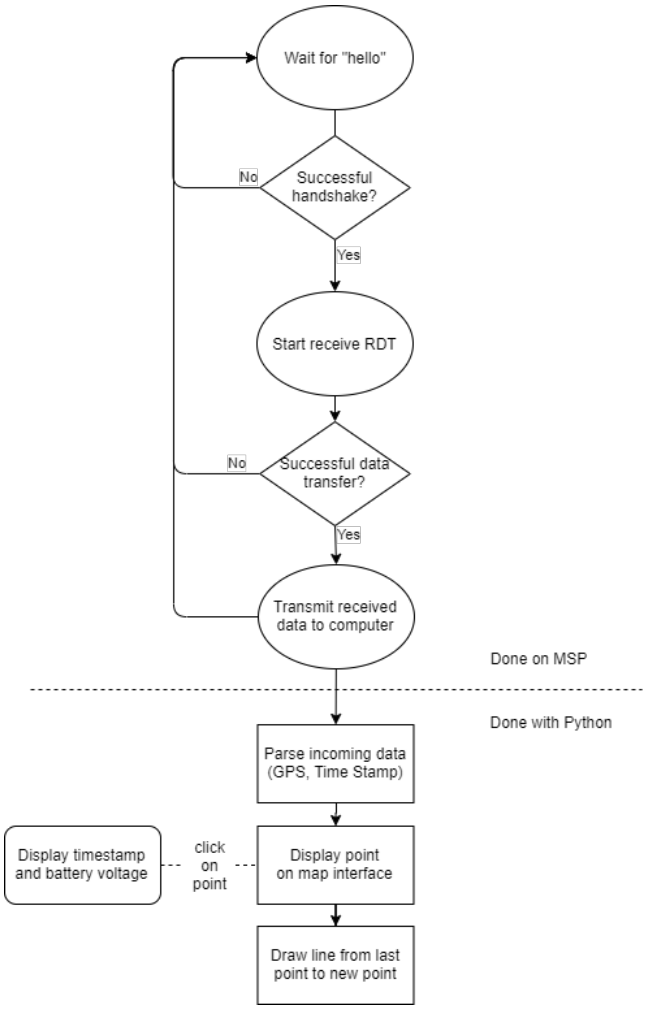

Figure 17: Home Node Firmware and Software Flow Diagram

Like the roaming node, the home node operates in an infinite loop. The home node first waits for a greeting message from the roaming node, which begins the handshake process of the RDT. Upon a successful handshake, the home node prepares to receive the data. If the data is received successfully, the home node transmits this data over UART to a computer. At each step of the wireless data reception process, there is an opportunity for failure. Failure can occur during the handshake and during the data transfer. In this scenario, the home node simply returns to waiting for a greeting message.

When the computer receives the data from the home node, it parses it into location coordinates and a time stamp. Using this information, it displays the roaming node's current location on a constantly updating map-based user interface. This interface shows a history of each roaming node's location, in the form of a drawn path. The user has the option to click on each roaming node's most recently recorded location, which will prompt the user interface to display the node's identification number and the time at which the node was at that location. For more information about the user interface, see the Detailed Technical Description: Software User Interface section of this report.

GPS

A SparkFun ZOE-M8Q GPS Breakout Board [41] gathers longitude, latitude, and time data. All of the programming for this portion of the project was done in embedded C using Code Composer Studio. The microcontroller communicates with the breakout board through SPI (serial peripheral communication) protocol. The breakout board provided pins for Master-Out-Slave-In (MOSI), Master-In-Slave-Out (MISO), Serial Clock (SCK), and Chip Select (CS). The breakout board also had the capability to use Inter-Integrated Circuit (I^2C) protocol to communicate with the MSP, but the team had more familiarity with SPI protocol from previous coursework, so SPI was chosen. To configure the GPS to use the SPI pins, D_SEL pin was grounded, found on the bottom of the breakout board. The serial clock frequency is 1 MHz.

The hardware setup was relatively straightforward for the GPS - the MSP was connected to the corresponding pins on the breakout board using jumper wires. As for configuring the GPS, the ZOE-M8Q outputs dummy data via UART when the chip is correctly configured. The GPS has a pin that corresponds to "Safeboot". When driven high, the GPS starts up and starts sending

dummy data. The output of the GPS will not be accurate, as the dummy data was just used to allow the user to know when the GPS has booted up and is ready to start receiving commands. To receive the dummy data, the Chip Select must be driven low before every SPI command that receives or sends bytes and driven high after the SPI command. For instance, when a 92-byte packet is being sent over SPI, the Chip Select must be driven low before any bytes are sent, then all 92 bytes must be sent, then Chip Select must be driven high.

Once the GPS was configured and dummy data was successfully received over SPI, a passive Molex Flexible GNSS antenna [63] was attached. An active antenna was previously used with our breakout board which caused the chip to heat up, so using a passive antenna proved to be very important. GPS data was sent and received using commands in UBX format [64]. This format gives a clear way to send data and check that received data is correct. The first command sent is “UBX-CFG”, which initializes the GPS SPI and sets the clock phase and polarity. Next, the program waits to receive a non-zero filled packet back from the GPS before moving on. Finally, the “UBX-NAV-PVT” command is sent, which requests data from the GPS and tells the GPS to lock on to a satellite and receive positional and time data. The GPS waits for a packet that has the first two bytes corresponding to 0xB5 and 0x62, which is how it knows that the data it is receiving is conforming to the UBX message format.

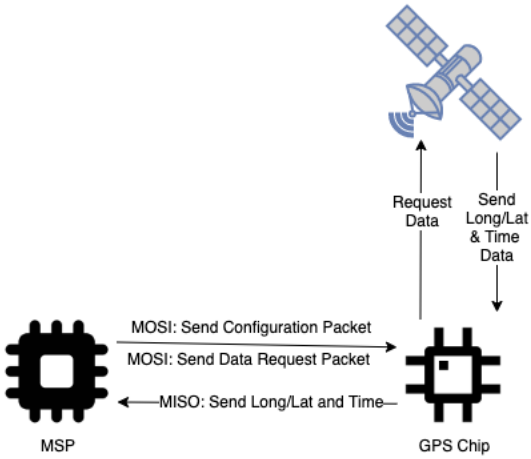

Figure 18. GPS Dataflow Diagram.

Upon successful reception of data from the satellite, the data is sent to MSP430 over SPI using the MISO port. When the MSP430 gets the packet containing all the data, it must parse out the longitude, latitude, hour, minute, second, day, and month. The parsed data is then fit into a payload of 15 bytes that is sent to the home node over LoRa. The interaction and dataflow for the MSP, GPS chip, and satellite can be seen in Figure 18. This process is done in an infinite while loop to ensure continuous GPS data reception.

LoRa Transceiver

The roaming node and home node communicate using LoRa modulation, implemented by the SX1262 LoRa transceiver [65]. LoRa transceivers use LoRa modulation, which is a chirp spread spectrum modulation scheme that trades data rate for sensitivity. During modulation, data is chipped at a high data rate and then modulated onto a chirp signal which continuously varies in frequency. The SX1262 LoRa transceiver operates in the 915 MHz band for the Fleet Tracker system. Also, it can have modulation bandwidths between 7.8 and 500 kHz, a spreading factor

between 5 and 12, and a bit rate between 0.018 - 62.5 kb/s. There is a tradeoff between sensitivity and data rate which are related by the following equation:

R_b= SF * 44+CR2SFBW,

where Rb is the bit rate, SF is the spreading factor, CR is the coding rate and BW is the modulation bandwidth. A higher spreading factor means better receive sensitivity but lower data rate, and a higher bandwidth means higher data rate and reduced sensitivity. Thus, to maximize range, the spreading factor was maximized at 12. To increase the data rate, reducing time-on-air and power consumption, the bandwidth was chosen to be 500 kHz. These parameters likely could have been better chosen to optimize range and reduce time-on-air. This is discussed in the Future Work section. Additionally, in order to further reduce the time-on-air, the payload of the LoRa data frame was chosen to be relatively small, as discussed in the Technical Description: Firmware: LoRa Protocol section. The coding rate is set to 1 to provide the best tradeoff between data rate and noise immunity. The bit rate is 37.5 kb/s [66].

The MSP430F5529 communicates with the LoRa transceiver using SPI, with a serial clock frequency of 1 MHz. All other parameters of the SPI communications including phase and polarity, were set according to the guidelines in the SX1262 datasheet. Using SPI, the MSP430F5529 sends commands to the LoRa transceiver based on the application programming interface (API) given by the transceiver manufacturer, Semtech. The datasheet details commands to configure and control the transceiver [65]. A library of C functions was implemented based on this information.

Before beginning normal operations, both the roaming node and home node must configure the transceiver using functions from the API. The configuration functions and parameters used for the Fleet Tracker are listed below.

- SetPacketType - LoRa packet
- SetRfFrequency - 915 MHz
- SetPaConfig
    - Duty cycle: 0x04
    - Power amplifier size: 0x07
- SetTxParams
    - Power: +22 dBm
    - Ramp time: 200 microseconds
- SetModulationParams
    - Header mode: implicit
    - Invert IQ mode: standard IQ
    - Preamble length: 12
    - Payload length: 15
    - CRC type: CRC on
- SetCadParams

- Number of symbols: 8
- Detection peak: 25
- Detection minimum: 6
- CAD exit mode: CAD only

The SX1262 LoRa transceiver has a number of known bugs and workarounds. Especially relevant to the Fleet Tracker system is the Implicit Header Mode Timeout Behavior issue, described in the transceiver datasheet. The team found experimentally that in implicit mode and with a spreading factor of 12, unexpected behavior occurs for the transceiver. The Fleet Tracker system implements the suggested workaround presented in the datasheet. A number of other known issues, less relevant to the Fleet Tracker system, are listed in the data sheet [65].

Finally, although the SX1262 LoRa Transceiver datasheet defines the LoRa payload buffer as being 256 bytes in size [65], other limitations restrict the usable size to 255 bytes. The configurations for LoRa frames are set using *LORA_SetPacketParams()*, which takes a payload length parameter. This parameter is maximum 8 bits in length, so the payload length can only range from 0 to 255 bytes. Thus, although the payload buffer is 256 bytes in size, the payload can only be configured to be up to 255 bytes. Attempting to configure the payload for 256 bytes will cause unintended behavior. Although the Fleet Tracker only uses a 15-byte payload, this information may be useful for future revisions.

LoRa Protocol

The SX1262 transceiver automatically handles functions related to the link layer LoRa frame. However, it does not utilize the proprietary medium access control (MAC) layer LoRaWAN protocol [67].

The link layer LoRa frame employed by the transceiver consists of a preamble, a header, a header cyclic redundancy check (CRC), a payload, and an optional payload CRC. For the Fleet Tracker, the transceivers all operate in implicit mode, in which the number of bytes and coding rate are implicitly known on both ends of the communication, and the header and its CRC are excluded. Additionally, the length of the preamble and the header are configurable through the transceiver application programming interface (API) [65].

The Fleet Tracker firmware does not explicitly handle the construction and deconstruction of the LoRa frame. Instead, the frame payload can be individually written and read directly using the 256-byte RAM data buffer. Additionally, the CRC errors are calculated within the LoRa chip, and they can be checked by reading the Interrupt Request (IRQ) register through the API [65].

Figure 19, from the Semtech SX1262 datasheet [65], shows the LoRa frame and its fields in explicit mode. In implicit mode, which the Fleet Tracker is using, the packet excludes the header and the header CRC fields.

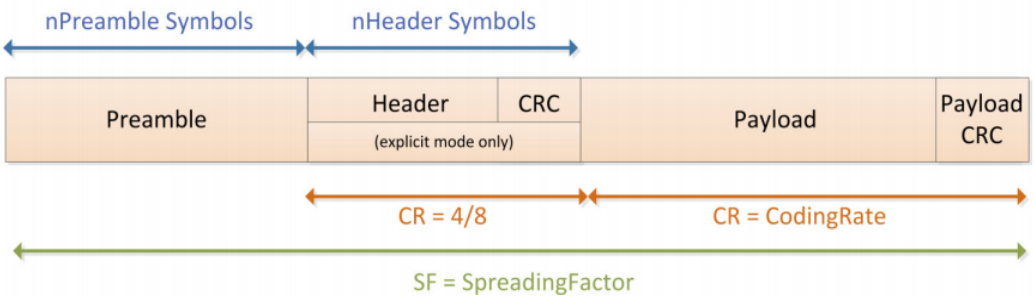

Figure 19. LoRa Frame (from Semtech SX1262 datasheet).

Reliable Data Transport Protocol

Above the LoRa link layer frame, the Fleet Tracker implements an original upper-layer reliable data transport (RDT) protocol. Using this protocol, the GPS and timestamp data are transmitted as a single packet. The protocol is designed to handle packet errors, dropped packets, and repeat transmissions through an acknowledgement system.

In total, each packet is 15 bytes long. This condensed packet size reduces the time-on-air for transmissions, reducing the power consumption of the transceiver. Each packet consists of a 1-bit sequence number, a 13-bit roaming node identification number (device ID), a 24-bit ADC reading, 78 bits of GPS data, and 4 unused bits. The 13-bit device ID, to which roaming nodes are uniquely assigned, allows for theoretically up to 8,192 roaming nodes to be present in a single Fleet Tracker network.

The GPS data itself contains several sub-fields. These are a 26-bit latitude, 26-bit longitude, 5-bit day value, 4-bit month value, 5-bit hour value, 6-bit minute value, and 6-bit second value. The number of bits allocated to each field of the GPS data was chosen to accommodate the expected range of each value. For example, with a range of month values from 0 to 11 representing January to December, four bits are necessary to fully represent the month information. Additionally, the latitude and longitude data are truncated from a 32-bit representation to a 26-bit representation. This design choice was made to improve the tradeoff between data accuracy and power consumption. This truncation reduced the data accuracy, but kept acceptable. However, it allowed for a more condensed payload size, which strongly influences the transmission time-on-air and reduces the power consumption of the system.

Figure 20 shows the Fleet Tracker packet structure and an accompanying breakdown of the GPS data. Note that this version of the Fleet Tracker does not fill the ADC field with valid data, as it does not implement firmware to read ADC values. However, the ADC field is present in the packet, and it can be filled with valid data in future revisions without altering the existing packet structure.

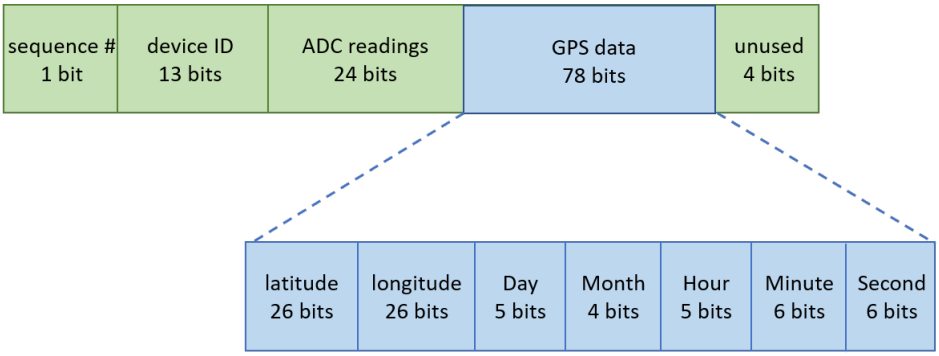

Figure 20: Fleet Tracker Packet

Each Fleet Tracker packet is wrapped into a LoRa Frame to be transmitted using LoRa modulation. In this layer wrapping, the Fleet Tracker packet acts as the payload of the LoRa frame. Figure 21 shows this layer wrapping.

Figure 21: Fleet Tracker (FT) Packet Wrapped in LoRa Frame

Note that there is no error checking within the Fleet Tracker packet itself. For simplicity, error checking is only handled only by the LoRa link layer, since the link layer frame wraps the Fleet Tracker packet.

Communication between a roaming node and home node is a two-step process. First, the roaming node and home node complete a handshake. Then, the roaming nodes transmits the data.

The handshake establishes a connection and allows the two nodes to trade information about the ensuing data transfer. The roaming node sends the home node its unique device ID, as well as the intended starting sequence number for the following data transfer. The device ID is necessary for the home node to differentiate between packets received from different roaming nodes. The starting sequence number is necessary because each distinct data transmission sequence, consisting of a handshake procedure and the data transfer itself, begins with a different sequence number, either 0 or 1. The handshake sequence is shown in Figure 22, in which the device ID is labeled *dev ID* and the starting sequence number is labeled *seq #*.

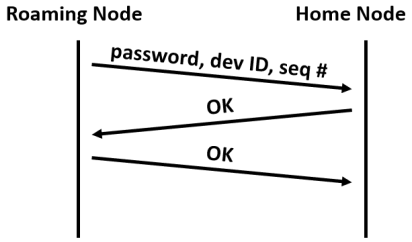

Figure 22: Protocol Handshake

This handshake procedure corresponds to the “Begin handshake” section of the Handshake sub-block for the roaming node firmware flow diagram discussed in the Technical Description: Firmware: General Firmware section. The Handshake sub-block is shown in Figure 23.

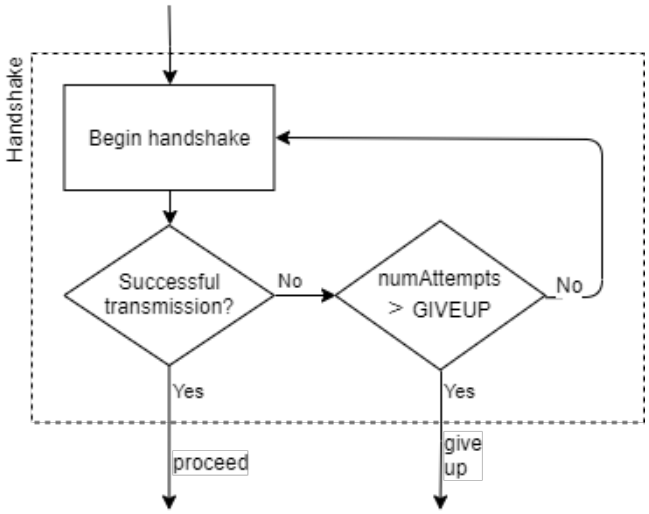

Figure 23: Roaming Node Firmware Handshake Sub-Block

After a successful handshake, the data transfer occurs. In this transfer, the roaming node transmits the LoRa frame, containing the Fleet Tracker packet, to the home node. This transfer is based on a sequence number and acknowledgement system. The transmitter sends a Fleet Tracker packet labeled with a sequence number of either a 0 or 1. Upon receiving a packet number with sequence number *x*, the recipient returns an acknowledgement (ACK) packet with the same sequence number *x*. Between successfully sent packets, the transmitter alternates sequence numbers. If the transmitter does not receive an acknowledgement before a preset timeout, the transmitter retransmits the original packet. With this acknowledgement system, no NACKs are necessary to indicate a failed packet transmission.

For this implementation, the timeout value was chosen to be 750 ms, based on the average time-on-air of a single packet transmission. Appendix A shows the calculations to estimate an average time-on-air of 264 milliseconds. The selected timeout value is about three times the time-on-air for a single packet, or one-and-a-half times the time to transmit a packet and receive and ACK.

Figure 24 shows the basic data transfer procedures dictated by the RDT protocol for a number of situations, including successful transmissions, lost packets, and repeated data.

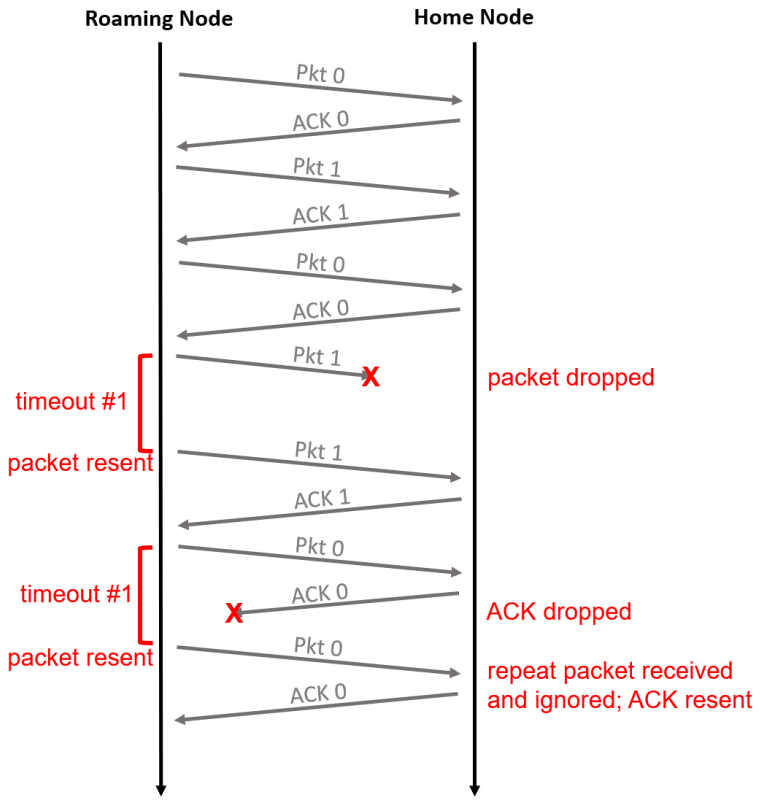

Figure 24: Fleet Tracker Reliable Data Transport Protocol

Similar scenarios occur if packets are received with errors. These errors could be CRC errors, which are checked in the LoRa link layer. These errors could also be a mismatch between the expected and received device ID, which is checked in the Fleet Tracker upper layer as part of the RDT protocol. If a Packet 0 is received with an error, the receiver will not return an ACK 0. The transmitter will time out and retransmit Packet 0. If Packet 1 is received without error, but ACK 1 is returned with error, the transmitter will resend Packet 1.

This data transfer procedure corresponds to the “Attempt transmission” section of the Transmit Data sub-block for the roaming node firmware flow diagram discussed in the Detailed Technical Description: Firmware: General Firmware section. The Transmit Data sub-block is shown in Figure 25. For this diagram, and unsuccessful transmission is the event that the roaming node receives an ACK with error or times out before receiving an ACK. This timeout could be caused by a lost packet, a lost ACK, or a packet received by the home node with error.

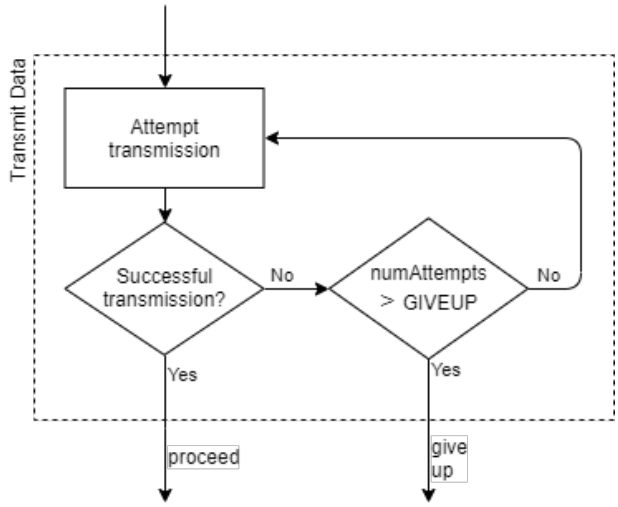

Figure 25: Roaming Node Firmware Transmit Data Sub-Block

Media Access Control Protocol

To avoid collisions, in which multiple roaming nodes simultaneously transmit data to the home node, and reduce data corruption, the Fleet Tracker network implements a multiple access control (MAC) protocol. Specifically, Carrier Sense Multiple Access (CSMA) with Collision Avoidance (CA) and exponential back-off is used. In this protocol, a transmitting node listens for activity on the channel in use. If no activity is detected, then the node proceeds with transmission [62]. Otherwise, it waits a period of time that exponentially increases with each attempt, then

transmits the data. After a specific number of failed attempts, the transmitting node “gives up” on transmitting the data.

For this version of the Fleet Tracker system, the exponential back-off was implemented using a base of 2. That is, after each successive failed attempt, the roaming node waits 2 seconds, then 4 seconds, then 8 seconds, and so on, until it gives up. This base value was chosen to be as low as possible, minimizing the rate of back-off as much as possible. During the wait time, the roaming node is active. Thus, a rapidly increasing wait time results in greater power consumption. Ultimately aiming to reduce power consumption as much as possible, a base value of 2 was chosen.

For the Fleet Tracker system, CSMA-CA was implemented using the SX1262 chip’s build-in Channel Activity Detection (CAD) functionality. This function senses the transmission channel for LoRa symbols, including both preamble and data symbols. Before the roaming node begins its standard operations, it must configure the CAD parameters for the LoRa transceiver. These parameters include the number of symbols that the CAD function uses, the minimum sensitivity, and the maximum sensitivity [65]. These values were chosen using Semtech’s SX126X CAD Performance Evaluation reference document. This document contains the experimentally determined best settings for CAD for a number of spreading factors, chosen to minimize the probability of a false detection. However, although the Fleet Tracker uses a spreading factor of 12, this document only lists the best CAD settings for spreading factors 7 through 11 [68]. Extrapolating from the given information and experimental tests, the Fleet Tracker CAD settings were set to be 8 symbols with a sensitivity range of +6 dBm to +25 dBm.

To use the CAD function, the interrupts for CadDone and CadDetected must be enabled. The LoRa transceiver can then be put in CAD mode. To determine the results of the sensing, the Interrupt Request (IRQ) status register must be read. Within this register, the CadDone flag will set when the chip has finished sensing the channel, regardless of whether activity was detected. The CadDetected flag is only set when activity has been detected on the channel. After reading the IRQ register, it must be cleared. The SX1262 datasheet details the processes for each of these steps [65].

Note that CSMA-CA does not eliminate the possibility of a collision, as transmission delays can cause a transmitter to falsely determine that a channel is quiet. This protocol also does not account for detecting collisions and recovering from them. However, CSMA-CA does reduce the probability of a collision, and the reliable data transfer protocol discussed above accounts for corrupted data. Although other multiple access protocols like TDMA and FDMA can completely eliminate collisions, these protocols were not chosen because they would require additional overhead, such as node synchronization and constant frequency retuning.

Software User Interface

A software program was written in Python to read the received payload from the home node via UART and display the route of each roaming node, with the software structure summarized in **Figure 26**. The Payload class divided the received payload, represented as a bit string, into the relevant subfields. The Map class had a single Fleet object, and upon receiving a Payload object would send this object to the Fleet class, which would check the Payload's device ID and add the object to the appropriate Entity in its list of Entities. Upon receiving a new payload, a map centered at the received GPS coordinate was loaded, and all Entities and their routes drawn,

saving the map to an HTML file before refreshing an Internet browser window with this file open.

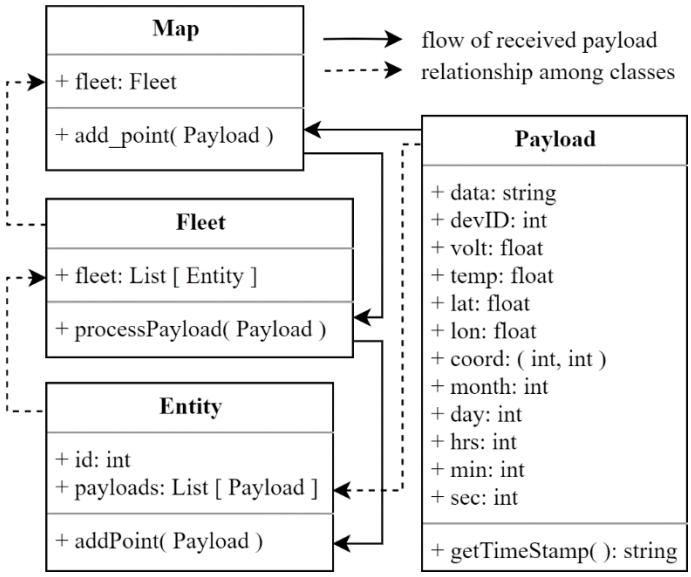

Figure 26. Software UML diagram.

Mechanical Casing

The chassis for the roaming nodes was carefully designed to follow existing weatherproofing conventions. The design began with a commercial electrical enclosure made of ABS plastic, with dimensions of 15.0 x 15.0 x 7.0 cm [16]. The enclosure is waterproof, with an IP rating of 65, meaning it is/has:

- Completely dust tight. Full protection against dust and other particulates, including a vacuum seal, tested against continuous airflow.
- Protection against low-pressure jets (6.3 mm) of directed water from any angle (limited ingress permitted with no harmful effects) [69, 17].

To attach the roaming node to the roof of a vehicle, a car roof suction cup was attached to the plastic enclosure [70]. The solar panel was affixed to the top of the plastic enclosure, and the LoRa antenna protruded from the side of the enclosure to limit interference of the enclosure walls with the radio communication. For all three protruding objects, circular holes were drilled into the enclosure, following the directions from [71] stating circular holes were the simplest to seal. Following directions from [72], an O-ring was used around the suction cup to further seal the enclosure. Finally, waterproof caulk was applied to the three enclosure openings to seal the design from the environment.

Problems and Design Modifications

The team experienced three major issues that led to design modifications. Two involved the design of the power system, and one involved the encryption of the data.

Initially, the team developed a separate PCB for the power system. This included the same battery charging IC (BQ24210) [47] but a different buck-boost regulator (TPS63031) [52] than is on the final board. Both of these chips are manufactured by TI and have specific TI footprints, the 10-WSON and the 10-VSON respectively. The team mistakenly thought that they were the same footprint, which resulted in the buck-boost shorting all pins to ground since the middle ground pad was larger for the 10-WSON than the 10-VSON. Since the footprint could not be modified on the power board, the board was abandoned, and the power section was added to the roaming node board. The team swapped the TPS636031 for the ISL91127IR 3.3V buck-boost regulator [58] since the standard QFN footprint would be easier to solder and debug. In addition to swapping the buck-boost regulator, the team added two current sensor ICs (ACS722LLCTR-20AB-T) [73] to the power system. However, the initial parts were meant for currents ranging

from 0 to 20A, and had 18mA of resolution, which introduced a lot of error since the active components draw 20-40mA. To mitigate this issue, the current sensors were replaced with a lower resolution (4mA) version (ACS722LLCTR-05-AB-T) [73]. This reduced noise on the power system demo and allowed for better verification of the power system.

Finally, while the code for AES was available well in advance of the project deadline, there were issues when it was integrated into the system. After some debugging, the team realized that the LoRa protocol relied on the sequence number and device ID within the payload remaining unchanged for authentication purposes, while the AES encryption algorithm modified all 120 bits of the data. Additionally, the AES function could only be called when transmitting the 120-bit payload containing GPS data, and not when sending an ACK message from the home node, since the message was shorter in length. However, as encryption was not part of the project's original deliverables and did not affect the system's performance, it was left as a future feature of the system.

Project Timeline

A free Gantt Chart tool was used to create a timeline of the project [74]. The initial timeline was modified during the Midterm Design Review, both shown in **Figure 27**, with key dates in red so the team would remain cognizant of Fall Break, the Midterm Design Review, Thanksgiving Break, and Demo Day. Each large category of tasks, such as the PCB, Network protocols, GPS firmware, Software UI, and Mechanical Chassis, were parallelized, while each subtask within these categories was serial, relying on successful past steps to continue. In particular, it was important to frontload ordering parts and designing the PCBs, since these had the longest turnaround times and the rest of the system relied on these tasks being completed. At the

Midterm Design Review, the team realized that each task took longer than expected, but all tasks were more parallelizable than anticipated, so the updated Gantt chart reflects the team's parallelization of tasks. Finally, system integration and testing were predicted to be time consuming, so all task deadlines were pushed up, with the team aiming to have a working system by Thanksgiving break. This deadline was met, resulting in a functional and mostly error-free system on demo day.

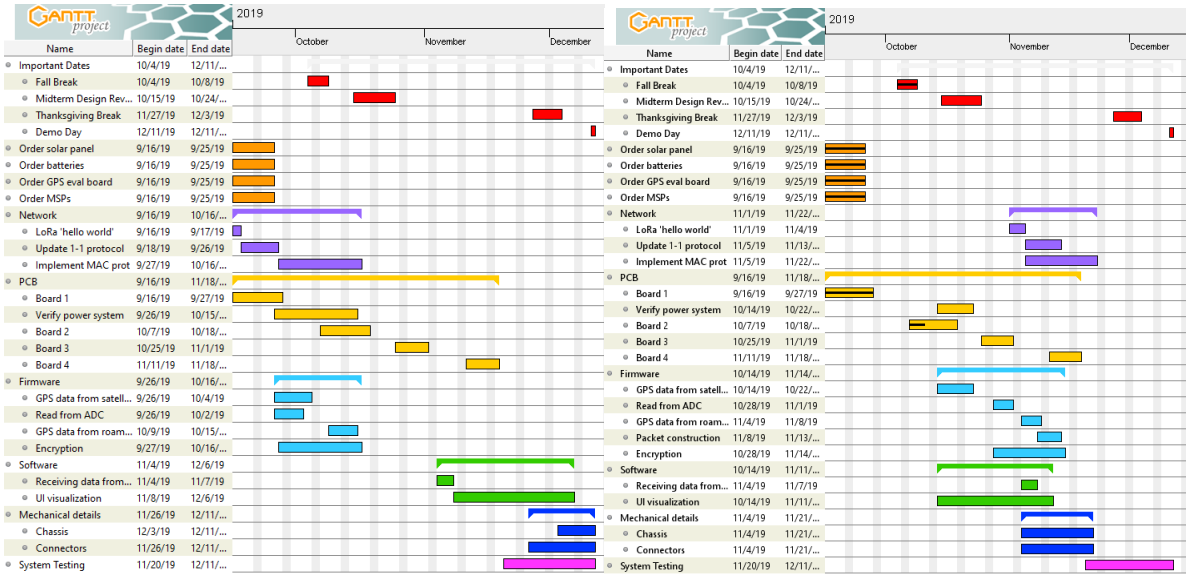

Figure 27. Original project timeline (left) and updated project timeline prior to Midterm Design Review (right)

Test Plan

The fleet tracker is divided into multiple systems that were each tested independently. This includes the hardware, the firmware, and the software. The firmware was tested using the prototyped system to isolate any errors from board design errors. The hardware was tested in various stages including the power system and the RF section.

The home and the roaming nodes were designed for complete debugging capabilities. Test pins and header pins allow for easy access of any node, including all SPI lines and all stages of the power system. This made it relatively simple to verify that the boards were designed and populated correctly. The PCBs were tested for correct connections, short circuits, and acceptable voltage levels while powered by a power supply. This was done using the connectivity check and DC voltage modes on a digital multimeter (DMM). Each of the four boards (1 home node, 2 roaming nodes, 1 power system) we produced were tested, and three passed all basic tests. The power system board did not supply the correct output power because of the footprint was wrong, which led to a redesign of the power system. This is explained in the Detailed Technical Description: Problems and Design Modifications section.

After its redesign, the power system was verified by measuring the power generated by the solar panel and the power drawn from the battery through four readings: the voltage at the battery terminal (to account for the inefficiencies of the solar charging IC), the voltage at VCC, the current entering the battery, and the current leaving the buck-boost 3.3V regulator. Those readings were sent to a myRIO, and LabVIEW was utilized to view the instantaneous power and the total energy consumed and produced. The LabVIEW system is explained in detail in Appendix D. This LabVIEW program was essential to verification of the roaming node power system, and was used to generate stable data to characterize the system under full sun to carry out the original test plan (shown in Figure 28).

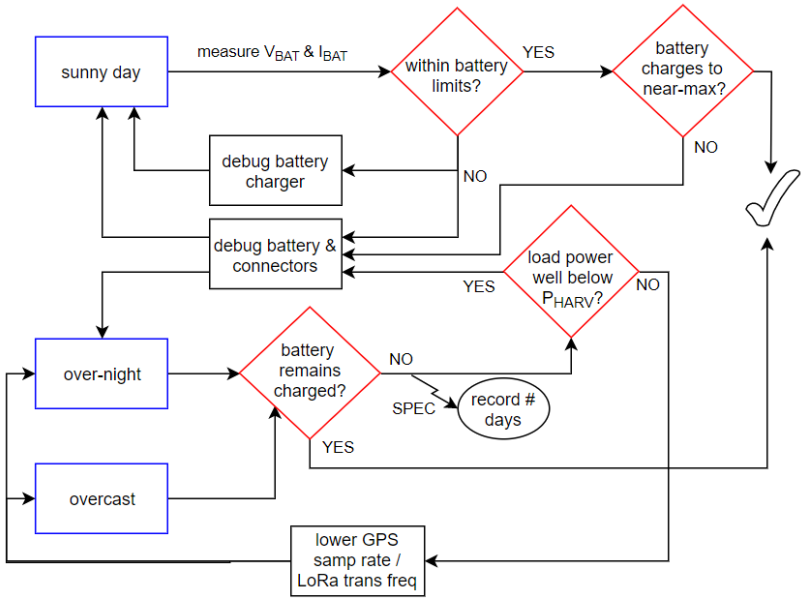

Figure 28: Power System Test Plan

A screenshot of the characterization data is shown in Figure 29. The input power is stable over time, with the solar panel delivering 1.33 W. The output power fluctuated over time due to transmissions, GPS acquisition, and duty cycling, but did not exceed 0.5 W. The number of days that the battery remains charge was not tested due to time constraints.

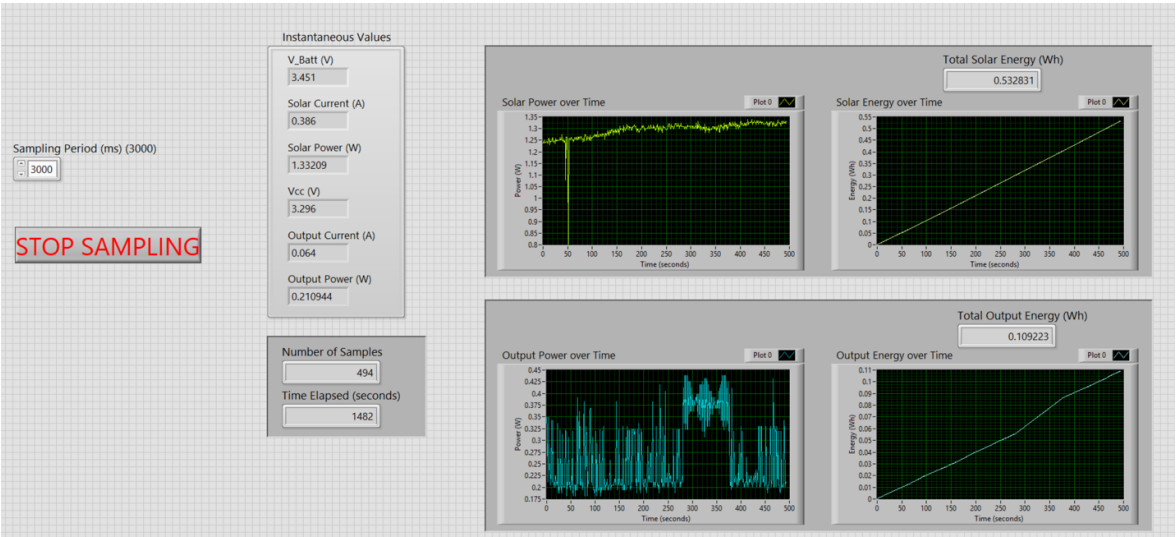

Figure 29: Roaming Node Power System Verification

The RF section of the home and roaming nodes was tested in the RF lab using a spectrum analyzer. The transceiver output was connected to the RF input using a 30 dB DC block. This attenuated the signal power by 30 dB. The spectrum analyzer was set to 915 MHz center frequency and 0 dB reference level. Two test functions exist to verify the RF section and the LoRa transceiver. The first, *LORA_SetTxContinuousWave()* tells the transceiver to output a steady, continuous wave at 915 MHZ with a power level of 22 dBm. This is shown in Figure 30. The second, *LORA_SetTXInfinitePreamble()* transmits an infinite preamble that appears as a peak continuously moving around 915 MHz. The home node and both roaming nodes passed both tests, displaying the appropriate RF output.

Figure 30: Continuous Wave RF Test

Once each node passed an individual power and RF test, the communication between them was verified. This was done using the functions *testTransmitOneFrame()* and *testReceiveOneFrame()* which allow for terminal-to-terminal communications between each node.

The test plan for the integrated system is shown in Figure 31, however it could not be carried out fully. Many factors limited full system testing. The first was range. The devices could only communicate if they were within a quarter mile, so no tests were performed with the roaming node attached to a car. Additionally, the GPS modules could not lock on to a satellite indoors, which affected the indoor demo. Finally, the UI required a Wi-Fi connection which limited the areas where the system could be tested. Due to those limiting factors, the first test block and the third test block could not be carried out, as the home node laptop was without Wi-Fi in a car, and the range was not great enough to perform the third test. Instead, the system was tested at a city park where the laptop could connect to a personal hotspot. Team members walked with the roaming nodes to demonstrate range and the MAC protocol. The chassis was tested by attaching it to the roof of a vehicle and driving on rough terrain.

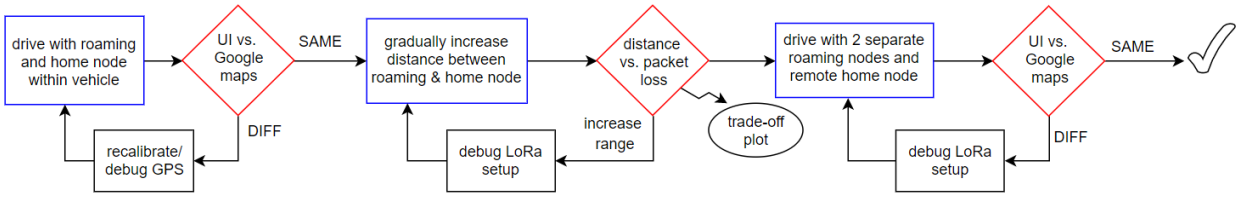

Figure 31: System Test Plan

Final Results

The team completed a fully functional system that tracks vehicles. This system contains all of the planned key components, including two solar-powered roaming nodes that gather GPS data, wireless data transmission using LoRa communications, and a stationary home node that visualizes received GPS data. More specifically, the system meets all of the four key criteria for success that were established in the project proposal, shown in Table 1. First, the two roaming

nodes each receive GPS data at a specified rate of one acquisition per five seconds. Second, this GPS data is wirelessly transmitted, and the reliable data transport protocol provides protections for timeouts, packet loss, and errors. Third, the GPS data from both nodes is displayed on a map-based user interface in real time. Fourth, the roaming node systems each receive power from a lithium ion battery that is charged while each device is actively operating. Thus, the final Fleet Tracker system fully satisfies all of the criteria for a fully functional system, placing it in the A grade range as defined by Table 2.

Points	**GPS Data Acquisition**	**GPS Data Transmission**	**GPS Data Visualization**	**Power**
3	GPS data is received from two modules at a specified rate	GPS data is wirelessly transmitted with protections for timeouts, packet loss, and errors	GPS data from multiple nodes is displayed on a map in real time	System runs from lithium ion battery that is charged by solar panel while device is operational
2	GPS data is received from a single module at a specified rate	GPS data is wirelessly transmitted without protections for	GPS data from a single node is displayed on a map in real time	System runs from lithium ion battery that can be charged by solar panel

		timeouts or packet loss		
1	GPS data is received from a single module	GPS data is transmitted over a wire	GPS data is printed out	System runs from Lithium Ion Battery
0	GPS data is not received from a module	GPS data is not transmitted	GPS data is not visualized	System requires wired power

Table 1. Grade Rubric.

Points	**Grade**
10 - 12	A
7 - 9	B
4 - 6	C
0 - 3	D

Table 2. Points to Letter Grade.

Despite this success, the team did not meet some of its additional goals. Although functional as a prototype, the design is not optimal and does not meet the expectations of a product in its market. One key drawback of the current design is the lack of data encryption. Although the team initially planned to use the Advanced Encryption Standard (AES) to encrypt the GPS data and increase security, this was not completed in time for the demonstration. Nayiri implemented AES

independently, but was unable to integrate it with the rest of the firmware. This was likely because other firmware components that were necessary for the integration were completed too late, leaving Nayiri with little time to successfully integrate the AES component. Additionally, the protocol and data transmission code were not modular enough that Nayiri could treat it as a black-box, making integration difficult.

The team also originally intended to take ADC readings of the roaming nodes' battery voltages and transmit them along with the GPS data. This would have been useful for ongoing testing and maintenance, even after the roaming nodes are deployed on vehicles. Since time was limited and this was not a core feature, the team chose to leave it out of the system. For similar reasons, the team chose not to implement "smart" duty cycling. This feature would have allowed the roaming node to dynamically calculate the optimal sleep time given the instantaneous harvested and stored energy.

Finally, the Fleet Tracker has only about a quarter mile of range. This limited range is likely because no team member has experience with RF concepts. As a result, naïve choices were made with respect to the transmission parameters and the choice of antenna.

This final result has taught the team a valuable lesson: Isolate the core functionality of the system, and set expectations accordingly. All additional features, such as the data encryption, ADC readings, and range, are important but secondary to the core functionality.

Costs

The cost of one fleet tracker system as was designed for this project with one home node and two roaming nodes is $463.22. A breakdown of costs at limited quantities and in high quantities is shown in Table 3.

Item	Quantity for 1 Fleet Tracker System	Cost per unit for 1 unit	Cost for 1 Fleet Tracker if 1 produced	Cost per unit for 10,000 units	Cost for 1 Fleet Tracker if 10,000 produced
Home Node PCB	1	$66.00	$66.00	$7.00*	$7.00
Home Node PCB Parts	1	$34.45	$34.45	$20.22	$20.22
Roaming Node PCB	2	$66.00	$66.00**	$8.89*	$17.78
Roaming Node PCB Parts	2	$70.35	$140.7	$34.46	$68.92
GPS Header Board	2	$44.95	$89.90	$44.95	$89.90
Chassis	2	$17.11	$34.22	$17.11	$34.22
Solar Panel	2	$8.99	$17.98	$8.99	$17.98

Battery	2	$6.99	$13.98	$4.50	$9.00
Total Cost			$463.22		$265.02

Table 3: Fleet Tracker Costs

*According to Advanced Circuits Custom Quote [75]

**If the two boards are panelized as they were during the production of this project

The most expensive part of the tracking system is the PCBs and their respective parts. Therefore, the cost decreases dramatically at high quantities. The 10,000-production unit cost is $264.76, almost $200, or 43% less expensive. These unit costs are based off of Advanced Circuit custom quotes for each board at large quantities (10,000 units) and the lowest unit cost from Digikey.com (5,000-1,000 units). A detailed spreadsheet of these reduced costs can be found in Appendix E. The above spreadsheet does not include the myRIO or the price of LabVIEW since they are not essential to a functioning system and are just used for testing. It also does not take the cost of prototyping into account, which added $88.24 to the total cost. The cost of assembly is unknown but use of a SMT pick-and-place machine will reduce assembly costs.

Future Work

To improve upon the current version of the Fleet Tracker, the team suggests implementing the four missing auxiliary features discussed in the Final Results section.

Future revisions should fully integrate the AES encryption into the data transfer process. When carrying out this task, care should be taken to accommodate the needs of the reliable data transport (RDT) protocol. AES encryption algorithm modifies all 128 bits of each packet

payload, including the sequence number and device ID. However, the RDT uses the sequence number and device ID to perform additional error checking. This was a major obstruction to Dugan's Dogs' progress on the AES component, and future teams should be aware of how the AES encryption interacts with the RDT protocol. Future revisions can also improve data security by implementing frequency hopping, which the SX1262 LoRa transceiver is capable of supporting [65].

As good practice, future teams should also implement the ADC readings component of the Fleet Tracker. Each roaming node should periodically take ADC readings of the battery voltage and transmit it along with the GPS and timestamp data to the home node. Making this information viewable in the user interface can improve the testability and maintainability of the system, even after the roaming nodes have already been placed on vehicles. The existing Fleet Tracker firmware already accounts for ADC data in the RDT protocol packet structure. Presently, roaming nodes send invalid data in the ADC field. However, future teams can easily fill this field with valid data without altering the packet structure.

To increase the robustness of the system, future revisions can implement "smart" duty cycling and retransmissions. By using smart duty cycling, or dynamically calculating the sleep time based on the instantaneous energy harvested and stored, the roaming nodes can extend their lifetimes even when the weather limits harvestable solar energy. Additionally, smart retransmissions offer an improved tradeoff between GPS sample frequency and power consumption. The roaming node firmware flow diagram, adjusted with smart duty cycling and a possible smart retransmissions scheme, is shown in Figure 32. In this smart retransmission scheme, represented in the sub-block Transmit Data, the roaming node decides whether to retransmit the packet based on how many consecutive previous successes and failures there were.

If the current packet fails and too many previous packets have also failed, then the roaming node will assume there exists some unavoidable problem in the communication channel, such as heavy traffic or range issues. It will give up and sleep for a long 10 minutes. If the current packet fails, but several of the recent packets have succeeded, the roaming node will assume that the loss of this packet would not be detrimental to the UI visualization. It will give up on this packet and dynamically calculate a short sleep time. This scheme reduces the number of unnecessary transmissions that the roaming node attempts, conserving power. It also considers how many GPS samples are necessary for the home node visualization to be considered real-time and accurate.

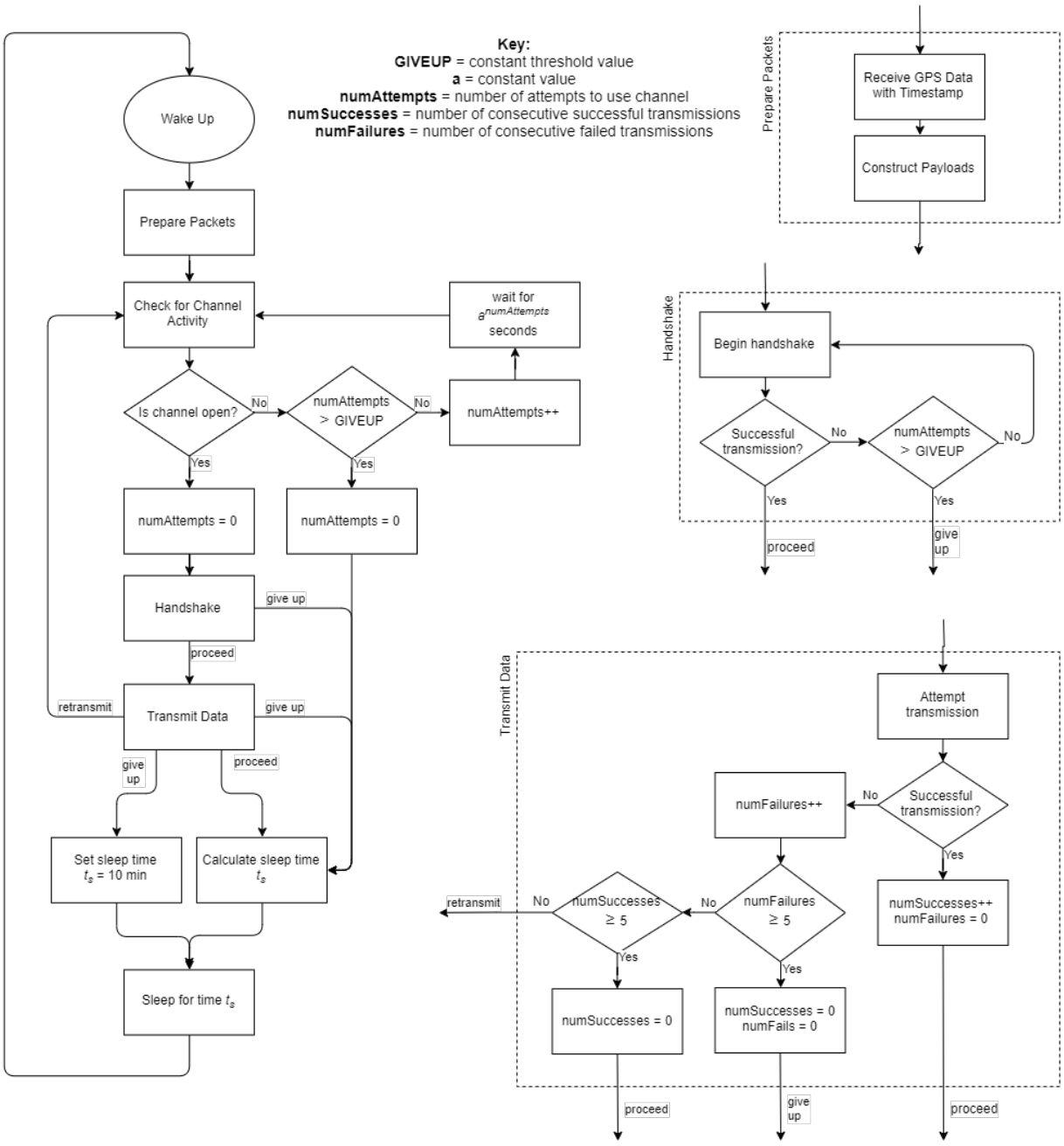

Figure 32: Roaming Node Firmware with Smart Duty Cycling and Retransmissions

Finally, before the Fleet Tracker can be mass produced and marketed, future revisions should improve the range of the data transfer. There are several ways to do this. First, a better choice of the transmission parameters may increase the range. The fundamental trade-off between

sensitivity and data rate in LoRa modulation makes this choice difficult, as this correlates between a trade-off between range and power consumption. However, detailed reference documents from the LoRa transceiver's manufacturer, Semtech, can provide guidance on the best choice of spreading factor, bandwidth, and coding rate.

Another method to increase the range is to more deliberately choose the antenna. The Fleet Tracker currently uses the 915 MHz antenna that came with the LoRa transceiver's development kit [76]. However, it is likely that this generic antenna is not optimized for the Fleet Tracker system, and an alternative would likely improve the range of the transmissions. The team suggests consulting with an expert well-versed in antenna design before making this choice.

Another more involved method to increase the range is to use Semtech's proprietary LoRaWAN media access control layer and network layer protocol. The Fleet Tracker system currently uses a peer-to-peer network architecture in a star topology. This limits the range of communications to the range of an individual Fleet Tracker node. In contrast, LoRaWAN can route LoRa frames between nodes that are separated by more than one "hop", extending the range of data transfer. LoRaWAN can also improve the scalability of the system [77].

References

[1] S. Li, L.D. Xu, and S. Zhao, "The Internet of Things: A survey," *Information Systems Frontiers*, vol. 17, no. 2, pp. 243-249, Apr. 2015, doi: 10.1007/s10796-014-9492-7. [Online].

[2] J. H. Nord, A. Koohang, and J. Paliszkiewicz, "The Internet of Things: Review and theoretical framework," *Expert Systems with Applications*, vol. 133, pp. 97-108, Apr. 2019, doi: 10.1016 /j.eswa.2019.05.014. [Online].

[3] W. R. da Silva, L. Oliveira, N. Kumar, R. A. L. Rabelo, C. N. M. Marins, and J. J. P. C. Rodrigues. (Dec. 9-13, 2018). An Internet of Things tracking system approach based on LoRa protocol. Presented at 2018 IEEE Global Communications Conference. [Online]. Available: https://ieeexplore.ieee.org/document/8647984

[4] J. M. Paredes-Parra, A. J. Garcia-Sanchez, A. Mateo, and A. Molina-Garcia, "An alternative Internet-of-Things solution based on LoRa for PV power plants: Data monitoring and management," *Energies*, vol. 12, no. 5, Mar. 2019, doi: 10.3390 /en12050881. [Online].

[5] F. Wu, C. Rudiger, and M. R. Yuce, "Real-time performance of a self-powered environmental IoT sensor network system," *Sensors*, vol. 17, no. 2, pp. 282, Feb. 2017, doi: 10.3390/s17020282. [Online].

[6] Samsara. "AG24." Samsara.com. https://www.samsara.com/products/models/ag24 (accessed Sep. 16, 2019).

[7] National Instruments. "myRIO Student Embedded Device." ni.com. http://www.ni.com /en-us/shop/select/myrio-student-embedded-device (accessed Dec. 16, 2019).

[8] Texas Instruments. "MSP430F5529." ti.com. https://www.ti.com/product/MSP430F5529?utm_source=google&utm_medium

https://www.ti.com/product/MSP430F5529?utm_source=google&utm_medium=cpc&utm_campaign=epd-null-null-GPN_EN-cpc-pf-google-wwe&utm_content=MSP430F5529&ds_k=%7b_dssearchterm%7d&DCM=yes&gclid=EAIaIQobChMI7bWqgae75gIVDG6GCh0KcA2mEAAYASAAEgLLmfD_BwE&gclsrc=aw.ds (accessed Dec. 16, 2019).

[9] National Instruments. "Multisim download." ni.com. https://www.ni.com/en-us/support/downloads/software-products/download.multisim.html#312060 (accessed Dec. 16, 2019).

[10] National Instruments. "Ultiboard download." ni.com. https://www.ni.com/en-us/support/downloads/software-products/download.ultiboard.html#311427 (accessed Dec. 16, 2019).

[11] Texas Instruments. "Code Composer Studio downloads." ti.com. http://software-dl.ti.com/ccs/esd/documents/ccs_downloads.html (accessed Dec. 16, 2019).

[12] Advanced Circuits. "2 & 4 layer PCB special pricing options." 4pcb.com. https://www.4pcb.com/pcb-prototype-2-4-layer-boards-specials.html (accessed Dec. 16, 2019).

[13] Operation within the bands 902-928 MHz, 2400-2483.5 MHz, and 5725-5850 MHz, Part 15.247, Federal Communications Commission, May 1, 2004 [Online]. Available: https://www.ecfr.gov/cgi-bin/text-idx?SID=766463bf6529cd6e086e707ba1ed43f8&mc=true&node=se47.1.15_1247&rgn=div8

[14] Operation within the bands 902-928 MHz, 2400-2483.5 MHz, 5725-5875 MHZ, and 24.0-24.25 GHz, Part 15.249, Federal Communications Commission, Feb. 1, 2012 [Online]. Available: https://www.ecfr.gov/cgi-bin/text-idx?SID=766463bf6529cd6e086e707ba1ed43f8&mc=true&node=se47.1.15_1249&rgn=div8

[15] Rhein Tech Laboratories, Inc., “EMC Regulatory Update,” Rheintech Laboratories, Inc., Feb. 2009. Accessed: Dec. 16, 2019. [Online]. Available: http://www.rheintech .com/images/multipoint/2009/MultiPoint-Regulatory-Update-February-2009.pdf

[16] Amazon. “LeMotech ABS plastic dustproof waterproof IP65 junction box universal electrical project enclosure white 5.9” x 5.9” x 2.8” (150mmx150mmx70mm).” amazon.com. https://www.amazon.com/dp/B075DG55KS?ref=ppx_pop_mob_ap_share (accessed Dec. 16, 2019).

[17] ANSI/IEC 60529-2004: Degrees of protection provided by enclosures (IP code): (identical national adoption), National Electrical Manufacturers Association, Nov. 3, 2004 [Online]. Available: https://www.nema.org/Standards/ComplimentaryDocuments /ANSI-IEC-60529.pdf

[18] IPC-2221A: Generic standard on printed board design, IPC: Association Connecting Electronics Industries, May 2003 [Online]. Available: http://www.ipc.org/TOC/IPC-2221A.pdf

[19] IPC-A-600F: Acceptability of printed boards, IPC: Association Connecting Electronics Industries, Nov. 1999 [Online]. Available: http://www.ipc.org/TOC/IPC-A-600F.pdf

[20] IPC-4101C: Specification for base materials for rigid and multilayer printed boards, IPC: Association Connecting Electronics Industries, Aug. 2009 [Online]. Available: http://www.ipc.org/toc/ipc-4101c.pdf

[21] Electronics Notes. “SMT / SMD components & packages, sizes, dimensions, details.” electronics-notes.com. https://www.electronicsnotes.com/articles/electronic_components/surface-mount-technology-smd-smt/packages.php (accessed Dec. 16, 2019).

[22] Electronics Notes. “USB Universal Serial Bus standards.” electronics-notes.com. https://www.electronics-notes.com/articles/connectivity/usb-universal-serial-bus/standards.php (accessed Dec. 16, 2019).

[23] Electronics Notes. “JTAG specification / IEEE 1149 standard.” electronics-notes.com. https://www.electronics-notes.com/articles/test-methods/boundary-scan-jtag-ieee1149/specification-standard.php. (accessed Dec. 16, 2019).

[24] SparkFun. “Serial communication.” sparkfun.com. https://learn.sparkfun.com/tutorials/serial-communication (accessed Dec. 16, 2019).

[25] Corelis. “SPI tutorial.” corelis.com. https://www.corelis.com/education/tutorials/spi-tutorial/ (accessed Dec. 16, 2019).

[26] RoHS Guide. “RoHS compliance FAQ.” rohsguide.com. https://www.rohsguide.com/rohs-faq.htm (accessed Dec. 16, 2019).

[27] Texas Instruments. “MSP driver library.” ti.com. http://www.ti.com/tool/MSPDRIVERLIB (accessed Dec. 16, 2019).

[28] The Open Group. “stdint.h - integer types.” opengroup.org. https://pubs.opengroup.org/onlinepubs/009695399/basedefs/stdint.h.html (accessed Dec. 16, 2019).

[29] The Open Group. “stdio.h - standard buffered input/output.” opengroup.org. https://pubs.opengroup.org/onlinepubs/7908799/xsh/stdio.h.html (accessed Dec. 16, 2019).

[30] The Open Group. “stdlib.h - standard library definitions.” opengroup.org. https://pubs.opengroup.org/onlinepubs/009695399/basedefs/stdlib.h.html (accessed Dec. 16, 2019).

[31] Digikey. “MSF-FET.” digikey.com. https://www.digikey.com/product-detail/en/texas-instruments/MSP-FET/296-37897-ND/4914406?WT.srch=1&gclid=Cj0KCQiA0NfvBRCVARIsAO4930k05cLjIgdYSZoQK8TXv7KdtBugxR1MQfp7xBYqCgNHPwVH2j-BXj4aAtf8EALw_wcB (accessed Dec. 16, 2019).

[32] Tera Term Open Source Project. “Tera Term home page.” ttssh2.osdn.jp. https://ttssh2.osdn.jp/index.html.en (accessed Dec. 16, 2019).

[33] Anaconda. “Python 3.7 version.” anaconda.com. https://www.anaconda.com/distribution/#windows (accessed Dec. 16, 2019).

[34] Anaconda. “Anaconda Cloud.” anaconda.com. https://anaconda.org/conda-forge/ (accessed Dec. 16, 2019).

[35] National Instruments. “LabVIEW.” ni.com. http://www.ni.com/en-us/support/downloads/software-products/download.labview.html?cid=Paid_Search-129008-US_Canada-Google_ESW1_Download_LV_Sitelinks&s_kwcid=AL!6304!3!277358336397!b!!g!!labview&gclid=EAIaIQobChMIvamhza255gIVWNyGCh1paQQNEAAYASABEgKQQPD_BwE#329059 (accessed Dec. 16, 2019).

[36] M. Shellenberger. “If solar panels are so clean, why do they produce so much toxic waste?” forbes.com. https://www.forbes.com/sites/michaelshellenberger/2018/05/23/if-solar-panels-are-so-clean-why-do-they-produce-so-much-toxic-waste/#158fa518121c (accessed Dec. 16, 2019).

[37] J. Gardiner. “The rise of electric cars could leave us with a big battery waste problem.” theguardian.com. https://www.theguardian.com/sustainable-business/2017/aug/10/electric-cars-big-battery-waste-problem-lithium-recycling (accessed Dec. 16, 2019).

[38] T. C. Frankel. “The cobalt pipeline: Tracing the path from deadly hand-dug mines in Congo to consumers’ phones and laptops.” washingtonpost.com. https://www .washingtonpost.com/graphics/business/batteries/congo-cobalt-mining-for-lithium-ion-battery/ (accessed Dec. 16, 2019).

[39] A. King. “Battery builders get the cobalt blues.” chemistryworld.com. https://www.chemistryworld.com/news/battery-builders-get-the-cobalt-blues/3008738.article (accessed Dec. 16, 2019).

[40] IMR Batteries. “Samsung 35E 18650 3500mAh 8A battery - Protected button top.” imrbatteries.com. https://www.imrbatteries.com/samsung-35e-18650-3500mah-8a-battery-protected-button-top/ (accessed Dec. 16, 2019).

[41] SparkFun. “SparkFun GPS breakout - ZOE-M8Q (Qwiic).” sparkfun.com. https://www .sparkfun.com/products/15193 (accessed Dec. 16, 2019).

[42] Digikey. “GPS-15193.” digikey.com. https://www.digikey.com/product-detail/en /sparkfun-electronics/GPS-15193/1568-GPS-15193-ND/10064427 (accessed Dec. 16, 2019).

[43] Corvil. “Discovering IoT devices and monitoring their network traffic.” corvil.com. https://www.corvil.com/blog/2018/discovering-iot-devices-and-monitoring-their-network-traffic (accessed Dec. 16, 2019).

[44] Haidar *et al*, “Vehicle information system,” U.S. Patent 9 990 781, Jun. 5, 2019.

[45] S. Pomerantz, C. Abraham, and D. A. Lundgren, “Satellite-positioning-system tracking device and method for determining a position of the same,” U.S. Patent 8 022 867, Sep. 20, 2011.

[46] J. R. Lee, H. S. Chiu, C. H. Hsu, H. Lee, and H. Chang, “Safety status sensing system and safety status sensing method thereof,” U.S. Patent 0139391, May 9, 2019.

[47] Texas Instruments. *Bq24210 800-mA, single-input, single-cell Li-Ion battery solar charger*. (2015). Accessed: Dec. 16, 2019. [Online]. Available: http://www.ti.com/lit/ds/symlink/bq24210.pdf

[48] Sun Power. "How much power can solar energy generate on a cloudy day?" sunpower.com. https://us.sunpower.com/blog/2019/05/09/how-solar-panels-work-cloudy-days (accessed Dec. 16, 2019).

[49] U.S. Naval Observatory. "Comparative lengths of days and nights." aa.usno.navy.mil. https://aa.usno.navy.mil/faq/docs/longest_day.php (accessed Oct. 13, 2019)

[50] Samsung SDI Company. *Specification of product for Lithium-ion rechargeable cell: Model name: INR18650-35E, v1.1.* (2015). Accessed: Oct. 13, 2019. [Online]. Available: https://www.imrbatteries.com/content/samsung_35E.pdf

[51] Texas Instruments. *MSP430F552x, MSP430F551x mixed-signal microcontrollers.* (2018). Accessed: Dec. 16, 2019. [Online]. Available: http://www.ti.com/lit/ds/symlink/msp430f5529.pdf

[52] Texas Instruments. *TPS6303x high efficiency single inductor buck-boost converter with 1-A switches.* (2015). Accessed: Dec. 16, 2019. [Online]. Available: http://www.ti.com/lit/ds/symlink/tps63030.pdf

[53] Digikey. "SX1262MB2CAS." digikey.com. https://www.digikey.com/products/en?keywords=SX1262MB2CAS (accessed Dec. 16, 2019).

[54] Future Technology Devices International Ltd. *UMFT234XF development module*. Accessed: Dec. 16, 2019. [Online]. Available: https://www.ftdichip.com/Support/Documents/DataSheets/Modules/DS_UMFT234XF.pdf

[55] Texas Instruments. *MSP430 hardware tools: User's guide*. (2018). Accessed: Dec. 16, 2019. [Online]. Available: http://www.ti.com/lit/ug/slau278ae/slau278ae.pdf

[56] Texas Instruments. "MSP430F5529 Launch Pad power consumption." ti.com. https://e2e.ti.com/support/microcontrollers/msp430/f/166/t/424823 (accessed Dec. 16, 2019).

[57] Semtech. "SX1262MB1CAS_915MHz_e428v03a_prod_folder." semtech.my.salesforce.com. https://semtech.my.salesforce.com/sfc/p/#E0000000JelG/a/2R0000001NLf/Ur9UYR7C6nCYXYxP3jt_sgCKkoFKAfQeg2bJubWBw1s (accessed Dec. 16, 2019).

[58] Renesas. *ISL91127IR: High efficiency buck-boost regulator with 4.5A switches*. (2016). Accessed: Dec. 16, 2019. [Online]. Available: https://www.renesas.com/us/en/www/doc/datasheet/isl91127ir.pdf

[59] Semtech. *Application note: reference design explanation*. (2019). Accessed: Dec. 16, 2019. [Online]. Available: https://semtech.my.salesforce.com/sfc/p/#E0000000JelG/a/2R000000HSQj/MmehlfBHMs5N326wBVRKw68_lEoDBCVcB71X7BUQXYY

[60] Bittele Electronics Inc. *Standard multi-layer PCB stackup*. (2012). Accessed: Dec. 16, 2019. [Online]. Available: https://www.7pcb.ca/Upload_file/Multi-layer-stack-up.pdf

[61] CVEL. "Microstrip impedance calculator." clemson.edu. https://cecas.clemson.edu/cvel/emc/calculators/PCB-TL_Calculator/microstrip.html (accessed Dec. 16, 2019).

[62] GeeksforGeeks. "Carrier Sense Multiple Access (CSMA)." geeksforgeeks.org. https://www.geeksforgeeks.org/carrier-sense-multiple-access-csma/ (accessed Dec. 16, 2019).

[63] SparkFun. "Molex flexible GNSS antenna - U.FL (adhesive)." sparkfun.com. https://www.sparkfun.com/products/15246 (accessed Dec. 16, 2019).

[64] U-blox. *U-blox 8 / u-blox M8: Receiver description: Including protocol specification.* Accessed: Dec. 16, 2019. [Online]. Available: https://www.u-blox.com/sites/default/files/products/documents/u-blox8-M8_ReceiverDescrProtSpec_%28UBX-13003221%29_Public.pdf#page=17&zoom=100,0,286

[65] Semtech. *SX1261/2: Long range, low power, sub-GHz RF transceiver*. (2019). Accessed: Dec. 16, 2019. [Online]. Available: https://media.digikey.com/pdf/Data%20Sheets/Semtech%20PDFs/SX1261-62_v1.2_Jun2019.pdf

[66] Semtech. *AN1200.22: LoRa Modulation basics.* (2015). Accessed: Dec. 16, 2019. [Online].

[67] LoRa Alliance. "What is the LoRaWAN specification?" lora-alliance.org. https://lora-alliance.org/about-lorawan (accessed Dec. 16, 2019).

[68] Semtech. *Application note: SX126x CAD performance evaluation*. (2018). Accessed: Dec. 16, 2019. [Online].

[69] The Enclosure Company. "IP rated enclosures explained." enclosurecompany.com. https://www.enclosurecompany.com/ip-ratings-explained.php (accessed Dec. 16, 2019).

[70] Amazon. "Erickson 01704 3" roof suction cup, (pack of 2)." amazon.com. https://www.amazon.com/dp/B000BKEBPY?ref=ppx_pop_mob_ap_share (accessed Dec. 16, 2019).

[71] A. Weiman. "Tips on waterproofing components in harsh environments." designworldonline.com. https://www.designworldonline.com/tips-on-waterproofing-components-in-harsh-environments/ (accessed Dec. 16, 2019).

[72] C. Brown. "Nothing gets in: Waterproof enclosure design 101 (and IP68)." fictiv.com. https://www.fictiv.com/blog/posts/nothing-gets-in-waterproof-enclosure-design-101-and-ip68 (accessed Dec. 16, 2019).

[73] Allegro Microsystems. *ACS722: High accuracy, galvanically isolated current sensor IC with small footprint SOIC8 package.* (2019). Accessed: Dec. 16, 2019. [Online]. Available: https://www.allegromicro.com/~/media/Files/Datasheets/ACS722-Datasheet.ashx

[74] Gantt Project. "Gantt chart." ganttproject.biz. https://www.ganttproject.biz/ (accessed Dec. 16, 2019).

[75] Advanced Circuits. "Start instant quote." 4pcb.com. https://www.4pcb.com/instant_quote/index.html (accessed Dec. 16, 2019).

[76] Semtech. "Semtech SX1262/SX1262 development kit." mouser.com. https://www.mouser.com/new/semtech/semtech-sx1261-sx1262-dev-kits/?gclid=EAIaIQobChMI2vfNxpu75gIVEXiGCh2qVA5TEAAYASAAEgJuF_D_BwE (accessed Dec. 16, 2019).

[77] Semtech. "LoRa & LoRaWAN: What is LoRa? What is LoRaWAN?" semtech.com. https://info.semtech.com/lora-and-lorawan (accessed Dec. 16, 2019).

[78] J. C. Liando, A. Gamage, A. W. Tengourtius, and M. Li, "Known and unknown facts of LoRa: Experiences from a large scale measurement study," *ACM Trans. Sensor Netw.,* vol. 0, no. 0, Nov. 2018. [Online]. Available: https://www.ntu.edu.sg/home/limo/papers/TOSN-LoRa.pdf

Appendix

Appendix A: Energy Calculations

LoRa Time-on-Air

coding rate = $\frac{4}{5}$; 16 bit CRC; 500kHz Bandwidth; Spreading Factor (SF): 12; Explicit Header

15 byte payload; 0 Symbol Header (using implicit mode); Coding Rate: $\frac{4}{5}$ ⇒CR = 1;

10 symbol preamble

$$N_{symbol} = N_{symbol\ preamble} + 4.25 + 8 +$$

$$ceil\left(\frac{max(8*N_{byte\ payload}+N_{bit\ CRC}-4*SF+8+N_{symbol\ header},0)}{4*SF}\right)*(CR+4)$$

$$= 10 + 4.25 + 8 + ceil\left(\frac{max(8*15+16-4*12+8,0)}{4*12}\right)*(1+4)$$

$$= 22.25 + (2)*5$$

$$= 32.25$$

$$ToA(in\ ms) = \frac{2^{SF}}{Bandwidth(in\ kHz)} * N_{symbol}$$

$$= 264.192\text{ms}$$

Expected Active Transceiving Time for one Packet

E_T = Expected active transceiving time for one packet

$P(F)$ = probability of failed transmission ≤ 0.42

$P(S)$ = probability of successful transmission ≥ 0.58

G = give up threshold = 5

T_{TO} = timeout time = 750 ms

T_{ToA} = time on air = 264 ms

Note: probabilities are based on research done at Nanyang Technological University [78]. Their LoRa network had a spreading factor of 12. Packets were transmitted at a distance of 3km from the receiver without line of sight in the middle of a densely populated urban area. They found a 23% packet loss rate with these configurations.

Additionally, a 1% packet error rate was used which was taken from the LoRa transceiver datasheet for a similar configuration.

The timeout time was selected to be significantly greater than $2 * ToA$

$$E_T = [P(F)]^G * G * T_{TO} + \sum_{i=0}^{G-1} [P(S)] * [P(F)]^i * (2 * T_{ToA} + i * T_{TO}) = 1057ms$$

Average Current Draw of LoRa Transmitter on Roaming Node

$E_T = 1057ms$

$I_{transmit} = 118mA(at\ 915MHz, 22dBm)$

$I_{receive} = 4.6mA$

$I_{standby} = 600nA\ (RC\ mode)$

Since the processor on the home node runs at 1MHz, the time between the home node receiving a message and transmitting and acknowledgement is negligible compared to the time on air and is thus treated as zero for the following calculations.

The roaming node is transmitting for half of the time a packet is being processed since the other half is spent receiving the acknowledgement message(s).

In normal operation, the roaming node transmits data every 15 seconds, thus that duty cycle is used in these calculations.

$$I_{avg-LoRa} = \frac{\left(\frac{1}{2}E_T\right)(I_{transmit}) + \left(\frac{1}{2}E_T\right)(I_{receive}) + (15 - E_T)\left(I_{standby}\right)}{15\ seconds} \approx 4.9mA$$

Appendix B: Thermal Analysis

Component	Min Operating Temperature (Degrees Celsius)	Max Operating Temperature (Degrees Celsius)
GPS Breakout Board	-40	85
Molex Antenna	-40	85
Msp430f5529	-40	85
LoRa board	-40	85
Lithium Ion Battery	0 (Charge), -10 (Discharge), -20 (Store)	45 (Charge), 60 (Discharge), 60 (Store)
Battery Charger	0	125
Voltage Regulator	-40	85
Thermistor	-50	110

Table 4. Thermal Analysis.

A thermal analysis was necessary to ensure the system performs under various conditions. As seen in Table 1, the main components affected by temperature are the battery charger and the lithium ion battery. At 0 degrees Celsius, these components do not perform well, and at 45 degrees Celsius that battery will not charge efficiently. These problems were addressed by using a commercial electrical enclosure made of ABS plastic, a material which is known for its insulating properties [16]. An industrial-grade, commercially available, weatherproof suction

cup, was used [70]. These products, along with weatherproof caulk and other materials, ensured that the boards would not be greatly affected by thermally extreme environments.

Appendix C: Bill of Materials

Home Node

Quantity	Description	RefDes	Vendor	Price	Manufacturer	Manufacturer Part No.	Vendor Part No.
3	CAPACITOR, 0.1µF	C1, C2, C8	Digikey	0.10	Samsung Electro-M	CL21B104MBCNNNC	1276-2450-1-ND
1	CAPACITOR, 10µF	C3	Digikey	0.19	KEMET	C0805C106K4PACTU	399-8012-1-ND
1	CAPACITOR, 0.47µF	C4	Digikey	0.36	Murata Eletronics	GRM21BR71H474KA88K	490-8319-1-ND
1	CAPACITOR, 2.2nF	C5	Digikey	0.10	KEMET	C0805C222K5RACTU	399-1151-1-ND
2	CAPACITOR, 0.22µF	C6, C7	Digikey	0.11	Samsung Electro-M	CL21B224KBFNNNE	1276-1093-1-ND
1	RESISTOR, 47kΩ	R1	Digikey	0.10	TE Connectivity Pas	CRGCQ0805J47K	A130144CT-ND
1	CAPACITOR, 47nF	C10	Digikey	0.10	Murata Electronics	GRM155R71C473KA01J	490-11420-1-ND
1	INDUCTOR, 4.7nH	L2	Digikey	0.18	Murata Electronics	LQW15AN4N7C00D	490-1139-1-ND
1	INDUCTOR, 2.5nH	L4	Digikey	0.22	Murata Electronics	LQW15AN2N5C00D	490-6798-1-ND
1	INDUCTOR, 47nH	L5	Digikey	0.17	Murata Electronics	LQW15AN47NJ00D	490-1154-1-ND
1	INDUCTOR, 9.1nH	L6	Digikey	0.18	Murata Electronics	LQW15AN9N1H00D	490-8444-1-ND
1	CAPACITOR, 470nF	C12	Digikey	0.13	Murata Electronics	GRM155R61A474KE15D	490-3264-1-ND
1	CAPACITOR, 47pF	C13	Digikey	0.10	TDK Corporation	C1005NP01H470J050BA	445-13803-1-ND
2	CAPACITOR, NC	C14, C20					
1	RESISTOR, 0Ω	R2	Digikey	0.10	Vishay Dale	CRCW04020000Z0ED	541-0.0JCT-ND
1	CAPACITOR, 3pF	C15	Digikey	0.10	Murata Electronics	GRM1555C1H3R0BA01D	490-6237-1-ND
1	CAPACITOR, 5.6pF	C16	Digikey	0.10	Murata Electronics	GRM1555C1H5R6CA01D	490-6250-1-ND
2	CAPACITOR, 39pF	C17, C24	Digikey	0.10	Murata Electronics	GRM1555C1H390JA01D	490-5871-1-ND
1	CAPACITOR, 1µF	C9	Digikey	0.10	Samsung Electro-M	CL05A105KP5NNNC	1276-1076-1-ND
1	INDUCTOR, 15µH	L1	Digikey	0.14	TDK Corporation	MLZ2012M150WT000	445-6397-1-ND
1	INDUCTOR, 15nH	L3	Digikey	0.18	Murata Electronics	LQW15AN15NH00D	490-6772-1-ND
1	CAPACITOR, 100nF	C11	Digikey	0.10	Murata Electronics	GRM155R71C104KA88D	490-3261-1-ND
2	CAPACITOR, 1.8pF	C18, C19	Digikey	0.10	Murata Electronics	GRM1555C1H1R8BA01D	490-6215-1-ND
1	CAPACITOR, 2.4pF	C21	Digikey	0.10	Murata Electronics	GRM1555C1H2R4BA01D	490-6228-1-ND
2	RESISTOR, 100Ω	R3, R4	Digikey	0.10	Vishay Dale	CRCW0402100RFKEDC	541-3962-1-ND
2	CAPACITOR, 1nF	C22, C23	Digikey	0.10	Murata Electronics	GRM155R61A102KA01D	490-6295-1-ND
2	CAPACITOR, 3.3pF	C25, C26	Digikey	0.10	Murata Electronics	GRM1555C1H3R3BA01D	490-6238-1-ND
1	MSP430f5529	U2	Digi-Key	7.33	Texas Instruments	MSP430F5529IPNR	296-27306-1-ND
1	PE4259	U3	Digi-Key	0.84	pSemi	1046-1077-1-ND	1046-1077-1-ND
1	SX1262MB2CAS	U4	Digi-Key	7.94	Semtech Corporati	SX1262IMLTRT	SX1262IMLTRTCT-ND
2	RESISTOR, 10kΩ	R5, R6	Digikey	0.10	Stackpole Electron	RNCP0805FTD10K0	RNCP0805FTD10K0CT-ND
4	RESISTOR, 330Ω	R8, R10, R	Digikey	0.10	Vishay Dale	CRCW0805330RJNEA	541-330ACT-ND
1	USB2UART	U5	Digi-Key	6.76	FTDI, Future Techn	UMFT234XF	768-1174-ND
1	HDR1X4	J5	Digi-Key	0.45	Sullins Connector S	PPTC041LFBN-RC	S7002-ND
1	HDR1X8	J4	Digi-Key	0.67	Sullins Connector S	PPPC081LFBN-RC	S7041-ND
4	LED, LED_red	LED1, LED	Digikey	0.29	Lite-On Inc.	LTST-C171KRKT	160-1427-1-ND
1	CRYSTAL_NX2016SA	U6	Digi-Key	0.64	NDK America, Inc.	NX2016SA-32M-EXS00A-CS06465	644-1300-1-ND
1	SMA_EDGE_MNT	U1	Digi-Key	3.79	Cinch Connectivity	142-0701-801	J502-ND

Figure 33: Home Node BOM

Roaming Node

Quantity	Description	RefDes	Vendor	Price	Manufacturer	Manufacturer Part No.	Vendor Part No.
1	CAPACITOR, 47nF	C10	Digikey	0.10	Murata Electronics	GRM155R71C473KA01J	490-11420-1-ND
1	INDUCTOR, 4.7nH	L2	Digikey	0.18	Murata Electronics	LQW15AN4N7C00D	490-1139-1-ND
1	INDUCTOR, 2.5nH	L4	Digikey	0.22	Murata Electronics	LQW15AN2N5C00D	490-6798-1-ND
1	INDUCTOR, 47nH	L5	Digikey	0.17	Murata Electronics	LQW15AN47NJ00D	490-1154-1-ND
1	INDUCTOR, 9.1nH	L6	Digikey	0.18	Murata Electronics	LQW15AN9N1H00D	490-8444-1-ND
1	CAPACITOR, 470nF	C12	Digikey	0.13	Murata Electronics	GRM155R61A474KE15D	490-3264-1-ND
1	CAPACITOR, 47pF	C13	Digikey	0.10	TDK Corporation	C1005NP01H470J050BA	445-13803-1-ND
1	RESISTOR, 0Ω	R2	Digikey	0.10	Vishay Dale	CRCW04020000Z0ED	541-0.0JCT-ND
1	CAPACITOR, 3pF	C15	Digikey	0.10	Murata Electronics	GRM1555C1H3R0BA01D	490-6237-1-ND
1	CAPACITOR, 5.6pF	C16	Digikey	0.10	Murata Electronics	GRM1555C1H5R6CA01D	490-6250-1-ND
2	CAPACITOR, 39pF	C17, C24	Digikey	0.10	Murata Electronics	GRM1555C1H390JA01D	490-5871-1-ND
1	CAPACITOR, 1µF	C9	Digikey	0.10	Samsung Electro-Mechanics	CL05A105KP5NNNC	1276-1076-1-ND
1	INDUCTOR, 15µH	L1	Digikey	0.14	TDK Corporation	MLZ2012M150WT000	445-6397-1-ND
1	INDUCTOR, 15nH	L3	Digikey	0.18	Murata Electronics	LQW15AN15NH00D	490-6772-1-ND
1	CAPACITOR, 100nF	C11	Digikey	0.10	Murata Electronics	GRM155R71C104KA88D	490-3261-1-ND
2	CAPACITOR, 1.8pF	C18, C19	Digikey	0.10	Murata Electronics	GRM1555C1H1R8BA01D	490-6215-1-ND
1	CAPACITOR, 2.4pF	C21	Digikey	0.10	Murata Electronics	GRM1555C1H2R4BA01D	490-6228-1-ND
2	RESISTOR, 100Ω	R3, R4	Digikey	0.10	Vishay Dale	CRCW0402100RFKEDC	541-3962-1-ND
2	CAPACITOR, 1nF	C22, C23	Digikey	0.10	Murata Electronics	GRM155R61A102KA01D	490-6295-1-ND
2	CAPACITOR, 3.3pF	C25, C26	Digikey	0.10	Murata Electronics	GRM1555C1H3R3BA01D	490-6238-1-ND
1	PE4259	U3	Digikey	0.84	pSemi	1046-1077-1-ND	1046-1077-1-ND
1	SX1262MB2CAS	U4	Digikey	7.94	Semtech Corporation	SX1262IMLTRT	SX1262IMLTRTCT-ND
4	RESISTOR, 330Ω	R8, R10, R11, R12	Digikey	0.10	Vishay Dale	CRCW0805330RJNEA	541-330ACT-ND
1	USB2UART	U5	Digikey	6.76	FTDI	UMFT234XF	768-1174-ND
1	PPTC041LFBN	J5	Digikey	0.45	Sullins Connector Solutions	PPTC041LFBN-RC	S7002-ND
1	TI-MSP430-HDR	J1	Digikey	0.32	On Shore Technology	302-S141	ED10522-ND
4	LED, LED_red	LED1, LED2, LED3, LEI	Digikey	0.29	Lite-On Inc.	LTST-C171KRKT	160-1427-1-ND
1	CRYSTAL_NX2016S	U6	Digikey	0.64	NDK America, Inc.	NX2016SA-32M-EXS00A-CS	644-1300-1-ND
1	SMA_EDGE_MNT	U1	Digikey	3.79	Cinch Connectivity Solutions Joh	142-0701-801	J502-ND
1	LED, LED_yellow	LED5	Digikey	0.31	Lite-On Inc.	LTST-C171KSKT	160-1428-1-ND
1	BQ24210DQCT	U8	Digikey	3.04	Texas Instruments	BQ24210DQCT	296-28738-1-ND
1	LED, LED_red	LED6	Digikey	0.29	Lite-On Inc.	LTST-C171KRKT	160-1427-1-ND
2	TermBlock-2	U9, U10	Digikey	0.71	TE Connectivity	282836-2	A98076-ND
2	CAPACITOR, 1µF	Cbat1, Cbus	Digikey	0.15	KEMET	C0805C105K4RACTU	399-1284-1-ND
1	RESISTOR, 787Ω	Riset	Digikey	0.10	Panasonic	ERJ-6ENF7870V	P787CCT-ND
1	RESISTOR, 21.5kΩ	RTh	Digikey	0.36	Panasonic	ERA-6AEB2152V	P21.5KDACT-ND
2	RESISTOR, 2kΩ	Rchg, Rpg	Digikey	0.36	Panasonic	ERA-6AEB202V	P2.0KDACT-ND
5	CAPACITOR, 0.1µF	C1, C2, C8, C29, C34	Digikey	0.10	Samsung Electro-Mechanics	CL21B104MBCNNNC	1276-2450-1-ND
3	CAPACITOR, 10µF	C3, C30, C33	Digikey	0.19	KEMET	C0805C106K4PACTU	399-8012-1-ND
1	CAPACITOR, 0.47µI	C4	Digikey	0.36	Murata Eletronics	GRM21BR71H474KA88K	490-8319-1-ND
1	CAPACITOR, 2.2nF	C5	Digikey	0.10	KEMET	C0805C222K5RACTU	399-1151-1-ND
2	CAPACITOR, 0.22µI	C6, C7	Digikey	0.11	Samsung Electro-Mechanics	CL21B224KBFNNNE	1276-1093-1-ND
1	RESISTOR, 47kΩ	R1	Digikey	0.10	TE Connectivity Passive Product	CRGCQ0805J47K	A130144CT-ND
1	MSP430f5529	U2	Digikey	7.33	Texas Instruments	MSP430F5529IPNR	296-27306-1-ND
2	RESISTOR, 10kΩ	R5, R6	Digikey	0.10	Stackpole Electronics	RNCP0805FTD10K0	RNCP0805FTD10K0CT-ND
1	ISL91127IR	U11	Digikey	2.98	Renesas Electronics America Inc	ISL91127IRNZ-T7A	ISL91127IRNZ-T7ACT-ND
1	INDUCTOR, 1µH	L8	Digikey	0.45	Murata Electronics	1277AS-H-1R0M=P2	490-10590-1-ND
2	CAPACITOR, 22µF	C27, C31	Digikey	0.47	KEMET	C0805C226M8PAC7800	399-12069-1-ND
2	ACS722	U12, U13	Digikey	5.27	Allegro	ACS722LLCTR-05AB-T	620-1634-1-ND
1	HDR1X8	J4	Digikey	0.67	Sullins Connector Solutions	PPPC081LFBN-RC	S7041-ND
1	myRIO_MXP	J9	Digikey	5.23	TE Connectivity	1-534206-7	A26466-ND
1	LiBatteryHolder	U7	Digikey	2.58	Keystone Electronics	1043P	36-1043P-ND
1	Antenna	N/A	Digikey	5.74	PulseLarsen Antennas	W1910	553-1699-ND

Figure 34: Roaming Node BOM

Quantity	Description	Price	Vendor	Manufacturer	Manufacturer Part Number
2	GPS Breakout Board	44.95	Digikey	SparkFun Electronics	GPS-15193
2	GPS Antenna	2.8	Digikey	Molex	2065600100
2	Electrical Enclosure	12.49	Amazon	LeMotech	lm201709071388
2	Suction Cup	4.62	Amazon	Erikson	Erickson 01704

Figure 35: Additional Parts BOM

Appendix D: LabVIEW Power System Verification Program

The highest-level Virtual Instrument (VI), main, consists of code to initialize, process data, and properly close the system. Error clusters were used to explicitly declare the execution of these three parts and to verify that the sampling and filtering values were valid. If the values input by the user are invalid, a simple error handler VI displays a message to the user, skips over the processing portion of the program and stops execution. The VI hierarchy is shown in Figure 36.

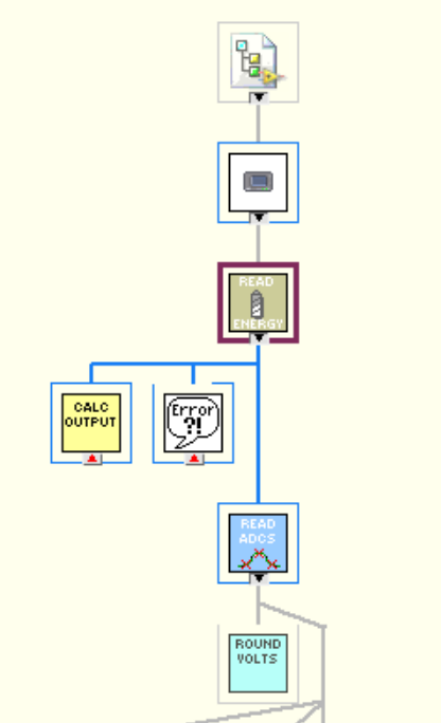

Figure 36: VI Hierarchy of LabVIEW Project (not including built in VIs)

The front panel of the main VI has controls to set the sampling period and to stop the sampling (which causes the main loop to exit). Additionally, the front panel displays the number of samples acquired, the total amount of time elapsed, the instantaneous values related to the input and output power and graphs of power and energy over time.

Figure 37: Main VI Front Panel

From the main VI, two subVIs are called: Read ADCS and Calculate Output. Read ADCS takes multiple samples from the 4 ADC channels and averages their values to reduce noise.

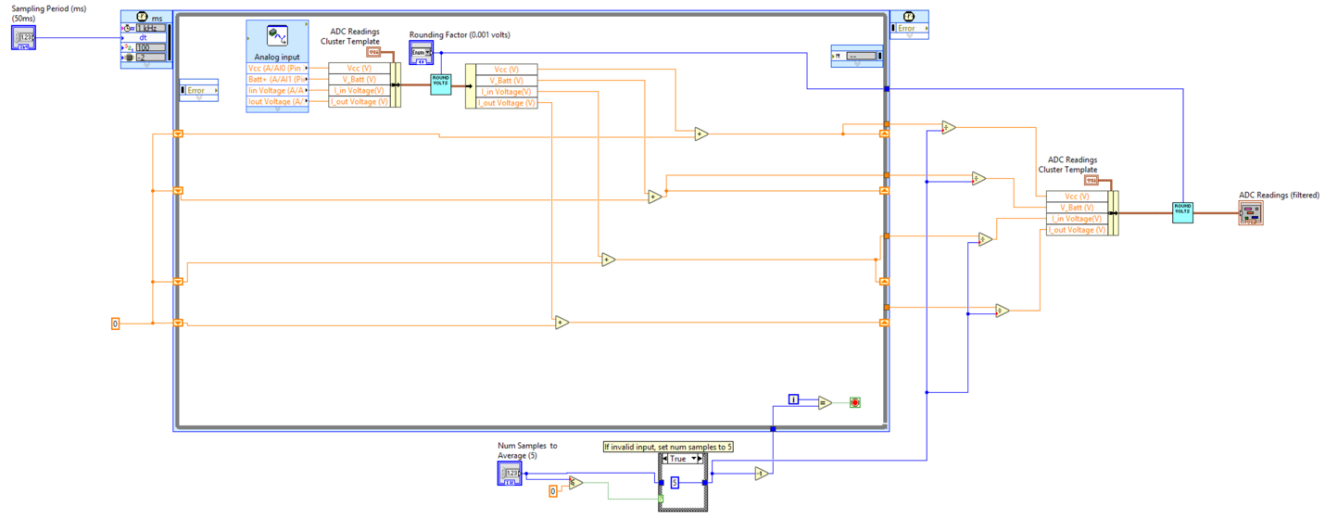

Figure 38: Read ADCs VI Block Diagram

The Calculate Output VI calls a VI to convert the voltage read from the hall effect into a current. Then, it performs power calculations.

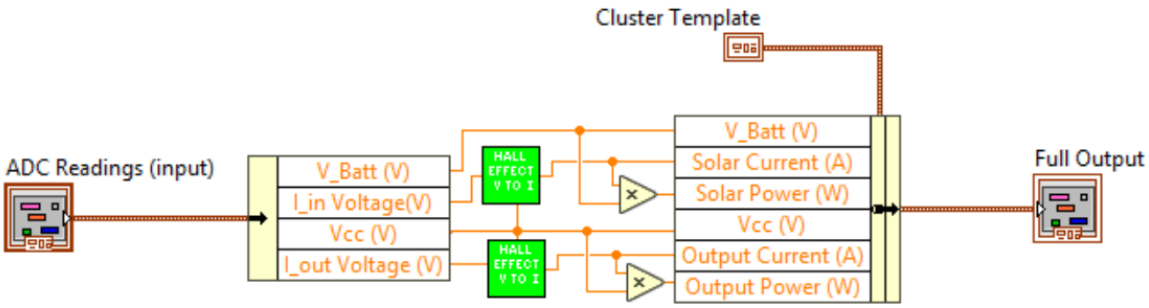

Figure 39: Calculate Output VI

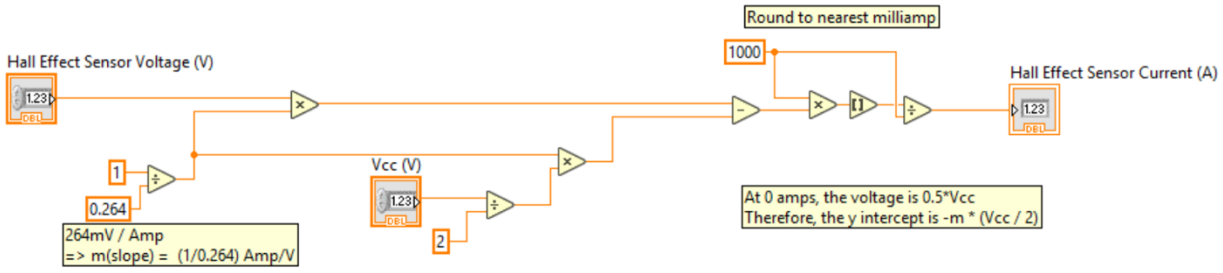

Figure 40: Conversion of Hall Effect Voltage to Current

To reduce jitter, all loops are timed using the myRIO's 1kHz clock. To maintain a consistent structure of data between VIs, clusters were used to transfer and display data.

Appendix E: Project Costs

Project total costs included prototyping, PCBs and parts orders and are outlined in Table 5. Prototyping included the purchase of two MSP430 launchpads, a LoRa evaluation board, and an antenna breakout board. All other costs are the same as outlined in the Costs section. The total project cost came to $597.83. Detailed spreadsheets showing the bulk discount for board parts are seen in Figures 41 and 42.

Item	Total Cost
Power Board Parts	$13.36
Power Board	$33
Prototyping	$88.24
Home Node PCB	$66.00
Home Node PCB Parts	$34.45
Roaming Node PCBs	$66.00
Roaming Node PCB Parts	$140.7
GPS Header Board	$89.90
Chassis	$34.22
Solar Panel	$17.98
Battery	$13.98
Total Cost	$597.83

Table 5: Project Total Costs

Quantity	Description	RefDes	Unit Price	Total Price	10,000 Unit Price	Total Price (10,000 unit price)
3	CAPACITOR, 0.1µF	C1, C2, C8	0.1	0.3	0.01029	0.03087
1	CAPACITOR, 10µF	C3	0.19	0.19	0.04015	0.04015
1	CAPACITOR, 0.47µF	C4	0.36	0.36	0.09071	0.09071
1	CAPACITOR, 2.2nF	C5	0.1	0.1	0.1361	0.1361
2	CAPACITOR, 0.22µF	C6, C7	0.11	0.22	0.02096	0.04192
1	RESISTOR, 47kΩ	R1	0.1	0.1	0.0058	0.0058
1	CAPACITOR, 47nF	C10	0.1	0.1	0.01189	0.01189
1	INDUCTOR, 4.7nH	L2	0.18	0.18	0.06522	0.06522
1	INDUCTOR, 2.5nH	L4	0.22	0.22	0.07789	0.07789
1	INDUCTOR, 47nH	L5	0.17	0.17	0.0621	0.0621
1	INDUCTOR, 9.1nH	L6	0.18	0.18	0.06522	0.06522
1	CAPACITOR, 470nF	C12	0.13	0.13	0.02176	0.02176
1	CAPACITOR, 47pF	C13	0.1	0.1	0.017631	0.017631
1	RESISTOR, 0Ω	R2	0.1	0.1	0.00654	0.00654
1	CAPACITOR, 3pF	C15	0.1	0.1	0.00403	0.00403
1	CAPACITOR, 5.6pF	C16	0.1	0.1	0.01164	0.01164
2	CAPACITOR, 39pF	C17, C24	0.1	0.2	0.00741	0.01482
1	CAPACITOR, 1µF	C9	0.1	0.1	0.00738	0.00738
1	INDUCTOR, 15µH	L1	0.14	0.14	0.00844	0.00844
1	INDUCTOR, 15nH	L3	0.18	0.18	0.06038	0.06038
1	CAPACITOR, 100nF	C11	0.1	0.1	0.06522	0.06522
2	CAPACITOR, 1.8pF	C18, C19	0.1	0.2	0.00688	0.01376
1	CAPACITOR, 2.4pF	C21	0.1	0.1	0.01164	0.01164
2	RESISTOR, 100Ω	R3, R4	0.1	0.2	0.00418	0.00836
2	CAPACITOR, 1nF	C22, C23	0.1	0.2	0.0061	0.0122
2	CAPACITOR, 3.3pF	C25, C26	0.1	0.2	0.01164	0.02328
1	DugansDogs, MSP430f5529	U2	7.33	7.33	4.77672	4.77672
1	DugansDogs, PE4259	U3	0.84	0.84	0.56	0.56
1	DugansDogs, SX1262MB2CAS	U4	7.94	7.94	4.46513	4.46513
2	RESISTOR, 10kΩ	R5, R6	0.1	0.2	0.01053	0.02106
4	RESISTOR, 330Ω	R8, R10, R11, R12	0.1	0.4	0.00632	0.02528
1	DugansDogs, USB2UART	U5	6.76	6.76	6.76	6.76
1	DugansDogs, PPTC041LFBN	J5	0.45	0.45	0.2041	0.2041
1	DugansDogs, PPPC081LFBN	J4	0.67	0.67	0.3042	0.3042
4	LED, LED_red	LED1, LED2, LED3, LED4	0.29	1.16	0.05306	0.21224
1	DugansDogs, CRYSTAL_NX2016SA	U6	0.64	0.64	0.33968	0.33968
1	DugansDogs, SMA_EDGE_MNT	U1	3.79	3.79	1.64	1.64
			Total Price	34.45		20.22336

Figure 41: Home Node Costs

Quantity	Description	RefDes	Unit Price	Total Price	10000 unit price	Total Price (10,000 unit)
1	CAPACITOR, 47nF	C10	0.1	0.1	0.01189	0.01189
1	INDUCTOR, 4.7nH	L2	0.18	0.18	0.06522	0.06522
1	INDUCTOR, 2.5nH	L4	0.22	0.22	0.07789	0.07789
1	INDUCTOR, 47nH	L5	0.17	0.17	0.0621	0.0621
1	INDUCTOR, 3.1nH	L6	0.18	0.18	0.06522	0.06522
1	CAPACITOR, 470r	C12	0.13	0.13	0.02176	0.02176
1	CAPACITOR, 47pF	C13	0.1	0.1	0.01731	0.01731
1	RESISTOR, 0□	R2	0.1	0.1	0.00403	0.00403
1	CAPACITOR, 3pF	C15	0.1	0.1	0.01164	0.01164
1	CAPACITOR, 5.6p	C16	0.1	0.1	0.00741	0.00741
2	CAPACITOR, 39pI	C17, C24	0.1	0.2	0.00738	0.01476
1	CAPACITOR, 1µF	C9	0.1	0.1	0.00844	0.00844
1	INDUCTOR, 15µH	L1	0.14	0.14	0.06038	0.06038
1	INDUCTOR, 15nH	L3	0.18	0.18	0.06522	0.06522
1	CAPACITOR, 100n	C11	0.1	0.1	0.00688	0.00688
2	CAPACITOR, 1.8pI	C18, C19	0.1	0.2	0.01164	0.02328
1	CAPACITOR, 2.4p	C21	0.1	0.1	0.00418	0.00418
2	RESISTOR, 100□	R3, R4	0.1	0.2	0.0061	0.0122
2	CAPACITOR, 1nF	C22, C23	0.1	0.2	0.0061	0.0122
2	CAPACITOR, 3.3p	C25, C26	0.1	0.2	0.01164	0.02328
1	PE4259	U3	0.84	0.84	0.56	0.56
1	SX1262MB2CAS	U4	7.94	7.94	4.46513	4.46513
4	RESISTOR, 330□	R8, R10, R11, R12	0.1	0.4	0.00623	0.02492
1	USB2UART	U5	6.76	6.76	6.76	6.76
1	PPTC041LFBN	J5	0.45	0.45	0.2041	0.2041
1	TI-MSP430-HDR	J1	0.32	0.32	0.1204	0.1204
4	LED, LED_red	LED1, LED2, LED3, LED4	0.29	1.16	0.05306	0.21224
1	CRYSTAL_NX201	U6	0.64	0.64	0.33968	0.33968
1	SMA_EDGE_MNT	U1	3.79	3.79	1.64	1.64
1	LED, LED_yellow	LED5	0.31	0.31	0.05652	0.05652
1	BQ24210DQCT	U8	3.04	3.04	2.12	2.12
1	LED, LED_red	LED6	0.29	0.29	0.05306	0.05306
2	TermBlock-2	U9, U10	0.71	1.42	0.21205	0.4241
2	CAPACITOR, 1µF	Cbat1, Cbus	0.15	0.3	0.02969	0.05938
1	RESISTOR, 787□	Riset	0.1	0.1	0.01045	0.01045
1	RESISTOR, 21.5k□	RTh	0.36	0.36	0.04536	0.04536
2	RESISTOR, 2k□	Rchg, Rpg	0.36	0.72	0.04536	0.09072
5	CAPACITOR, 0.1µI	C1, C2, C8, C29, C34	0.1	0.5	0.01029	0.05145
3	CAPACITOR, 10µF	C3, C30, C33	0.19	0.57	0.04015	0.12045
1	CAPACITOR, 0.47	C4	0.36	0.36	0.03071	0.03071
1	CAPACITOR, 2.2n	C5	0.1	0.1	0.01361	0.01361
2	CAPACITOR, 0.22	C6, C7	0.11	0.22	0.02096	0.04192
1	RESISTOR, 47k□	R1	0.1	0.1	0.0058	0.0058
1	MSP430f5529	U2	7.33	7.33	4.77672	4.77672
2	RESISTOR, 10k□	R5, R6	0.1	0.2	0.01053	0.02106
1	ISL91127IR	U11	2.98	2.98	2.077	2.077
1	INDUCTOR, 1µH	L8	0.45	0.45	0.19062	0.19062
2	CAPACITOR, 22µI	C27, C31	0.47	0.94	0.1372	0.2744
2	ACS722	U12, U13	5.27	10.54	2.24895	4.4979
1	HDR1X8	J4	0.67	0.67	0.3042	0.3042
1	myRIO_MXP	J3	5.23	5.23	3.0305	3.0305
1	LiBatteryHolder	U7	2.58	2.58	1.52	1.52
1	Antenna	N/A	5.74	5.74	2.7265	2.7265
			Total Price	70.35		37.50419

Figure 42: Roaming Node Costs